AD-A130 756 HEAT CHECKING IN THE CONTACT ZONE OF A FACE SEAL (A THREE-DIMENSIONAL MOD..(U) NEW MEXICO UNIV ALBUQUERQUE DEPT OF MECHANICAL ENGINEERING F D JU ET AL. APR 83 1/1

UNCLASSIFIED ME-121(83)ONR-414-2 N00014-76-C-0071 F/G 12/1 NL

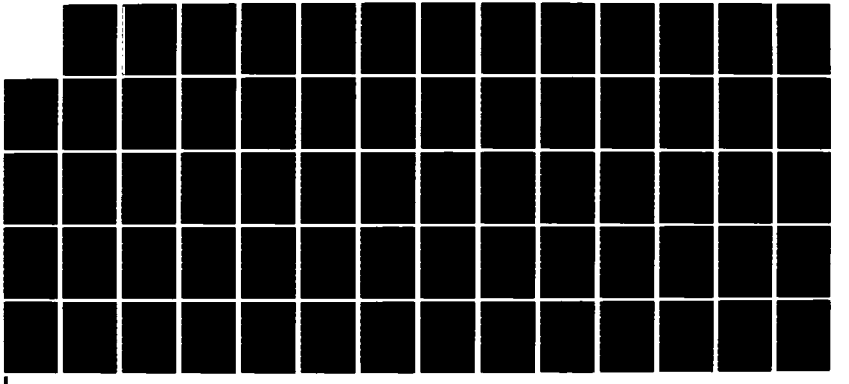

END

FILMED

DTIC

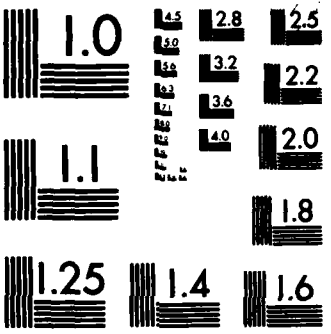

MICROCOPY RESOLUTION TEST CHART
NATIONAL BUREAU OF STANDARDS-1963-A

AD A130756

THE UNIVERSITY OF NEW MEXICO
COLLEGE OF ENGINEERING

BUREAU OF ENGINEERING RESEARCH

HEAT CHECKING IN THE CONTACT ZONE OF A FACE SEAL (A THREE-DIMENSIONAL MODEL OF A SINGLE MOVING ASPERITY)

BY

FREDERICK D. JU
JOHN H. HUANG

DTIC
ELECTE
JUL 27 1983

REPORT NO. ME-121(83)ONR-414-2

WORK PERFORMED UNDER CONTRACT NO. ONR-N00014-76-C0071

APRIL 1983

This document has been approved for public release and sale; its distribution is unlimited.

DTIC FILE COPY

83 07 15 001

Annual Report

on

HEAT CHECKING IN THE CONTACT ZONE OF A FACE SEAL (A THREE-DIMENSIONAL MODEL OF A SINGLE MOVING ASPERITY)

by

Frederick D. Ju
John H. Huang

Department of Mechanical Engineering
The University of New Mexico
Albuquerque, New Mexico 87131

Report No. ME-121(83)ONR-414-2
Work Performed Under Contract No. ONR-N00014-76-C-0071

April 1983

TABLE OF CONTENTS

ABSTRACT

Heat checking phenomenon in mechanical seals resulting from the passages of a single asperity over the face of a seal ring has been solved with a thermomechanical model of a semi-infinite medium subjected to the frictional heat source over the moving contact zone. An earlier analysis of such a problem was based upon a two-dimensional model of a single moving asperity. Such a load resulted in fracture which is initiated beneath the surface at the trailing edge of the moving load. For a better description of the physical problem, a three-dimensional model is examined in the present study. A single moving asperity, with a circular or a rectangular geometry of the contact area, is assumed on the mating part of the seal face. The general solution is obtained for any distribution of contact loads. Numerical solutions are obtained for uniform and parabolic distributions of pressure over the circular and rectangular contact zones. The traverse speed of the friction load is considered the same as the rubbing speed for the current problem. The roles of material properties and operating variables are delineated in terms of dimensionless parameters. The analytical solutions of the mechanical and the thermal stress fields are solved by means of the double Fourier transforms. The temperature field is obtained by the use of the Green's functions. Numerical results of the corresponding integral solutions are represented in graphs.

DTIC COPY INSPECTED 2

Accession For
NTIS GRA&I
TAB

Nomenclature

a	Asperity characteristic dimension, the half width of the rectangular contact area in the direction of traverse or radius of the circular contact area
b	Half length of the rectangular contact area perpendicular to the direction of traverse
c	specific heat
D	Differential operator with respect to x_3
k	Thermal conductivity
M_1	Dilatational speed ratio $[=V(\rho/(\lambda + 2\mu))^{1/2}]$
M_2	Shear speed ratio $[=V(\rho/\mu)^{1/2}]$
p_o	Average pressure over the contact area
q	Heat flux through the contact area
q_o	Average heat flux through the contact area $(=\mu_f p_o V)$
R_i	Traction over the contact area
t	Aspect ratio (b/a) or time
T	Temperature field
$\{u_i\}$, $\underset{\sim}{u}$	Displacement field
V	Traverse speed of asperity ($-x_1$ direction)
$\{x_i\}$	Coordinates fixed to the moving asperity
$\bar{(\ )}$	Fourier transform of a variable
∂_i	Partial derivative with respect to x_i coordinate
α	Coefficient of thermal expansion
δ_{ij}	Kronecker delta
ϕ	Dimensionless temperature field $(=Tk/q_o a)$
κ	Thermal diffusivity

λ	Lamé coefficient
μ	Lamé coefficient, modulus of rigidity
μ_f	Coulomb coefficient of friction
ρ	Mass density
σ_{ij}	Stress field
σ^*_{ij}	Dimensionless stress field
σ^M_{ij}	Mechanical stress field
σ^T_{ij}	Thermal stress field
$\{\xi,\eta,\zeta\}$	Dimensionless coordinates ($= x_i/a$)

LIST OF FIGURES

1.0 INTRODUCTION

The present investigation addresses one specific failure mechanism in marine seals, that severely affects its service life. The seal is designed to locate along the propeller shaft to prevent leakage of sea water through the shaft tunnel. Figure 1 illustrates one assembly of such device, in which the seal consists essentially of two mating annular rings, one of which is fixed to the tunnel housing, another is mounted under spring pressure to rotate with the shaft. The mating surfaces of the rings therefore are pressed against each other and rubbing at a high speed. The design nominal pressure between the seal rings depends on the type of vessel and the location of the seal. For instance, a low pressure of about 100 kPa (14.5 psi) is sufficient for most surface vessels; for submarines, the pressure required could increase by orders of magnitude. Had the pressure been evenly distributed according to design, the life of the seal will no longer be a serious problem even at a high rubbing speed. However, it is well-known that the actual contact area may only be a small fraction of the nominal area at the design interface. In other words, a low nominal design pressure may very well result in a very high interfacial pressure, thus a very high dry frictional force in the actual contact area. The high friction would cause locally an extremely high temperature, called "flash temperature" by Archard [1]. The local contact area is therefore otherwise called the "hot spot" [2]. In severe cases the temperature can be extremely high, leading to cracking of the surface [3]. The frictional cracking, or heat checking, has been observed to occur in seal rings [4]. If we use the figure of 10^{-3} as area ratio (contact area/nominal area)--Burton [5] considered 10^{-4} as a possible area ratio, a low pressure of 240 kPa (35 psi) could result in a 240 MPa (35000 psi) local pressure in the contact zone, a pressure well within the range of fracture initiation with unfavorable Coulomb coefficients [6].

The cause of the localization of the contact area will not be considered here; nor will the metallurgical change in the surface layer.

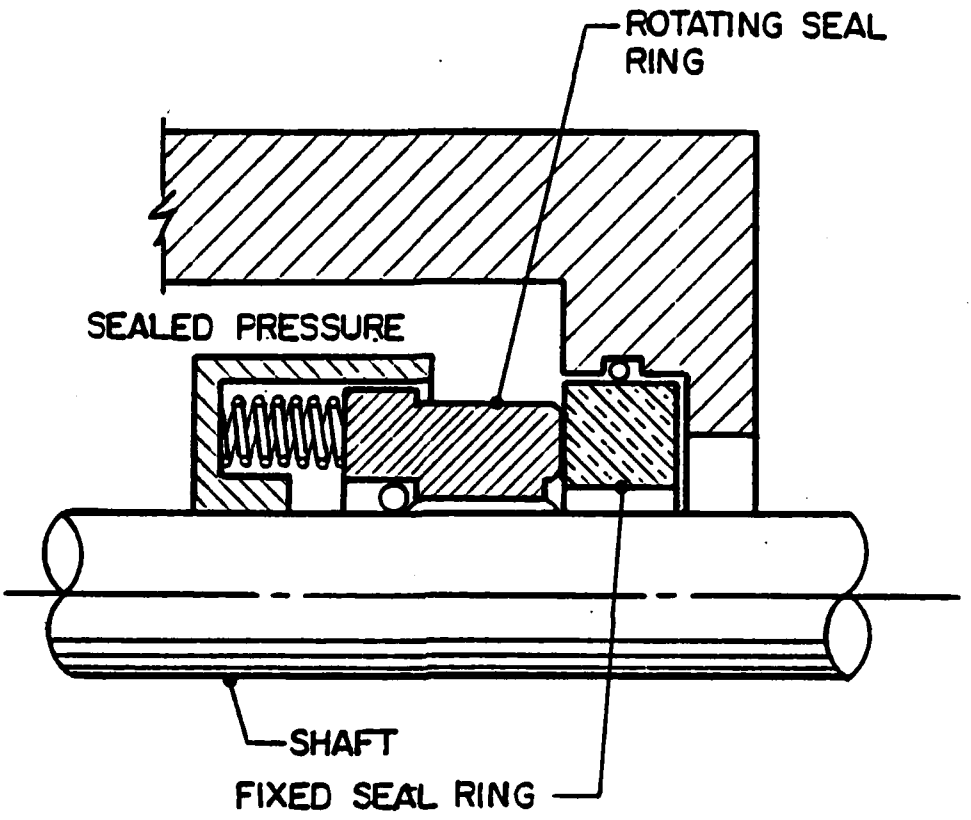

Figure 1. Mechanical face seal.

It will suffice to assume that the localization of contact areas is due to some form of asperities, which may be fixed to any of the mating surfaces or may precess with respect to both. Kennedy et al. [7], using carbon ring against a metallic mating ring of 440 Cs.s, beryllium copper or 52/00 bearing steel, showed existence of spot asperities on the metallic rings. Burton [8] reported on the use of aluminum ring on glass disk, showing hot spot precessing at a much slower speed compared to the rubbing speed. Marscher [9,10] treated the thermomechanical stress state in the part that contains the asperity. The present investigation treats the thermomechanical stress state in the part that mates with the one containing the asperity and the possibility of heat checking therein. The formulation also allows extension to problems of different rubbing speed and precessing speed of the asperity.

Because of the relative size of the seal material and the moving asperity, the seal will be represented by a half space. The asperity contacts with the material at the otherwise traction-free surface in a small rectangular or circular region, which traverses the surface at a speed (V) of the order of 10 m/s (~400 ips), Figure 2. The coordinates $\{x_i\}$ are fixed to the moving asperity such that x_1 points toward the trailing direction of the motion, x_2 is perpendicular to the traversing direction, and x_3 is a depth measure pointing inward from the surface into the material, Figure 2. For the rectangular contact area, the aspect ratio, $t(= b/a)$, is a parameter for three-dimensional effect. For large aspect ratio, the load is effectively a moving line load that has been represented by a two-dimensional plane strain solution [6]. In the present report the pressure and tangent force are arbitrarily distributed over the contact area for the general solutions in the integral form. Numerical solutions will be obtained specifically for the uniform and the symmetrical parabolic distributions.

Since the speed of traverse is much smaller than the Rayleigh wave speed, which for a steel based seal material is approximately 2800 m/s ($\sim 11 \times 10^4$ ips), no wave propagation phenomenon is considered. However, for the same material and a half contact width of the order of

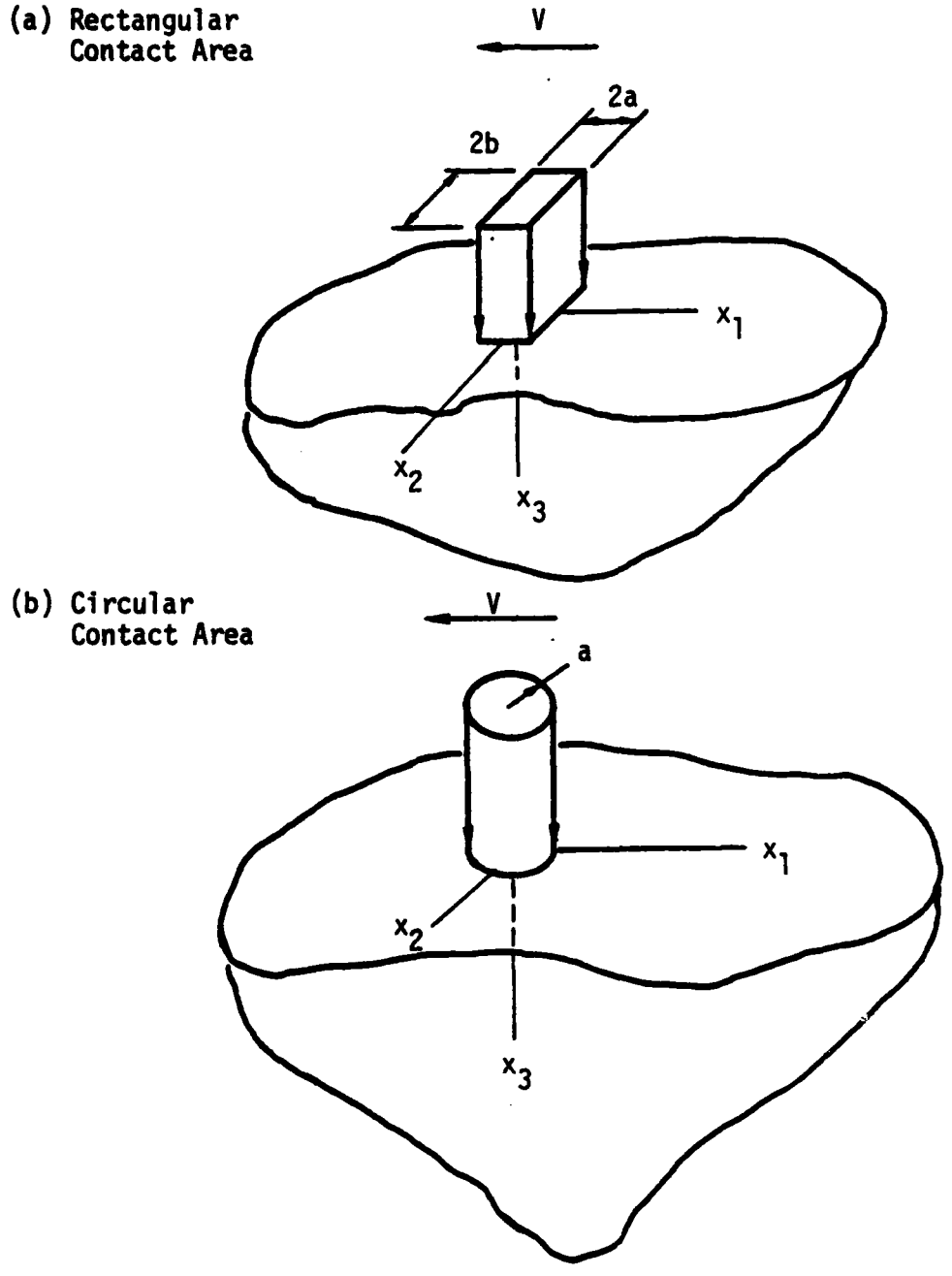

Figure 2. Moving asperities.

1 mm, the Peclét number ($Pe = Va/\kappa$) is of the order of 500, of which the magnitude is quite sufficient to necessitate the consideration of the dynamic effect of the traverse speed. It is assumed that the material remains predominantly elastic and hence that the uncoupled theory of thermoelasticity holds. Later it will be verified that the maximum principal stress will be under the yield stress except at a very small neighborhood where the ultimate strength is reached. The postulations allow us to treat the mechanical stress state and the thermal stress state separately. The combined effect will then determine the possibility of fracture initiation. The general solutions for the mechanical stress state, the temperature field and the thermal stress state are derived with the Fourier transform method and the Green's function method. The numerical data are computed with a combination of analytical integration and numerical method to avoid heavy computation time and stability problems.

2.0 STRESSES FROM MECHANICAL EXCITATION $\{\sigma^M_{ij}\}$

Basic Governing Equations. The working equations come from Cauchy's law and Hooke's law. In terms of the moving convective coordinates $\{x_i\}$ and with the absence of body forces, the acceleration in Cauchy's law will have only the convective terms. Hence, we have

$$\partial_j \sigma^M_{ij} = \rho V^2 \partial_{11} u_i \ , \tag{1}$$

$$\sigma^M_{ij} = \lambda \partial_k u_k \delta_{ij} + \mu(\partial_i u_j + \partial_j u_i) \ , \qquad i,j,k = 1,2,3 \tag{2}$$

where u_i is the displacement field, σ^M_{ij} is the mechanical stress field, ∂_j denotes partial derivative with respect to x_j, δ_{ij} is the Kronecker delta, V is the asperity traverse speed, (ρ, λ, μ) are material constants. The method to solve (1) and (2) will be similar to the one used by Eason [11].

Equations (1) and (2) are conveniently solved by the method of double Fourier transform with respect to (x_1, x_2)

$$\overline{f}(\overline{x}_1,\overline{x}_2,x_3) = \frac{1}{2\pi} \int_{-\infty}^{\infty} \int_{-\infty}^{\infty} f(x_1,x_2,x_3)\, e^{i(\overline{x}_1 x_1 + \overline{x}_2 x_2)}\, dx_1\, dx_2 \ . \tag{3}$$

With the use of the relation

$$\overline{\partial_r^n f} = (-i\,\overline{x}_r)^n\, \overline{f} \ , \quad r = 1,2 \ ,$$

we get

$$-i\overline{x}_r\, \overline{\sigma}^M_{jr} + D\, \overline{\sigma}^M_{j3} = -\rho V^2\, \overline{x}_1^2\, \overline{u}_j \ , \qquad j = 1,2,3 \ ; \ r = 1,2 \ , \tag{4}$$

---

[1] Summation convention is used for repeated indices of roman minuscules.

$$\left.\begin{aligned} \bar{\sigma}^M_{rs} &= -i\lambda\, \bar{x}_k \bar{u}_k \delta_{rs} - i\mu(\bar{x}_r \bar{u}_s + \bar{x}_s \bar{u}_r) + \lambda D\bar{u}_3 \delta_{rs} \\ \bar{\sigma}^M_{3r} &= -i\mu \bar{x}_r \bar{u}_3 + \mu D\bar{u}_r \\ \bar{\sigma}^M_{33} &= -i\lambda \bar{x}_k \bar{u}_k + (\lambda + 2\mu)\, D\bar{u}_3 \end{aligned}\right\} k,r,s = 1,2\ , \qquad (5)$$

subject to the boundary conditions

$$\bar{\sigma}^M_{3i} = -\bar{R}_i \quad \text{at} \quad x_3 = 0 \qquad (6)$$

and

$$\bar{u}_i \to 0 \quad \text{as} \quad x_3 \to \infty\ , \qquad (7)$$

where the transformed quantities are denoted by a superposed ($\bar{\ }$). R_i is the traction on the surface $x_3 = 0$, D denotes derivative with respect to x_3 and the index i = 1,2,3.

Displacement and Stress Fields. Solution of the set of ODE (4,5) follows by combining (4) and (5) first, resulting in

$$\begin{aligned} &[D^2 + (M_2^2 - \beta^2)\, \bar{x}_1^2 - \bar{x}_2^2]\, \bar{u}_1 - \bar{x}_1\bar{x}_2(\beta^2 - 1)\, \bar{u}_2 - i\bar{x}_1(\beta^2 - 1)\, D\bar{u}_3 = 0 \\ &-\bar{x}_1\bar{x}_2(\beta^2 - 1)\, \bar{u}_1 + [D^2 + (M_2^2 - 1)\, \bar{x}_1^2 - \beta^2\bar{x}_2^2]\, \bar{u}_2 - i\bar{x}_2(\beta^2 - 1)\, D\bar{u}_3 = 0 \\ &-i\bar{x}_1(\beta^2 - 1)\, D\bar{u}_1 - i\bar{x}_2(\beta^2 - 1)\, D\bar{u}_2 + [\beta^2 D^2 + (M_2^2 - 1)\, \bar{x}_1^2 - \bar{x}_2^2]\, \bar{u}_3 = 0 \end{aligned} \qquad (8)$$

in which

$$M_1 = V\left(\frac{\rho}{\lambda + 2\mu}\right)^{1/2} ; \qquad M_2 = V\left(\frac{\rho}{\mu}\right)^{1/2} ; \qquad \beta^2 = (\lambda + 2\mu)/\mu .$$

Equation (8) is a system of three simultaneous homogeneous linear equations for three unknowns $\{\bar{u}_i\}$. For nontrivial solutions the determinant of coefficients should be zero identically, that is

$$\Delta = \begin{vmatrix} D^2 + (M_2^2-\beta^2)\,\bar{x}_1^2 - \bar{x}_2^2 & -\bar{x}_1\bar{x}_2(\beta^2-1) & -i\bar{x}_1(\beta^2-1)\,D \\ -\bar{x}_1\bar{x}_2(\beta^2-1) & D^2 + (M_2^2-1)\,\bar{x}_1^2 - \beta^2\,\bar{x}_2^2 & -i\bar{x}_2(\beta^2-1)\,D \\ -i\bar{x}_1(\beta^2-1)\,D & -i\bar{x}_2(\beta^2-1)\,D & \beta^2 D^2 + (M_2^2-1)\,\bar{x}_1^2 - \bar{x}_2^2 \end{vmatrix}$$

$$= \beta^2(D^2 - n_1^2)\,(D^2 - n_2^2)^2 = 0 ,$$

where

$$n_r = (\bar{x}_1^2 + \bar{x}_2^2 - M_r^2\bar{x}_1^2)^{1/2} , \quad r = 1,2 .$$

Hence, Equation (8) results in

$$(D^2 - n_1^2)\,(D^2 - n_2^2)^2\,(\bar{u}_1, \bar{u}_2, \bar{u}_3) = 0 \tag{9}$$

whose solutions, with the consideration of the regularity condition (7), are

$$\bar{u}_1 = A_1 e^{-n_1 x_3} + (B_1 + C_1 x_3)\, e^{-n_2 x_3} ,$$

$$\bar{u}_2 = A_2 e^{-n_1 x_3} + (B_2 + C_2 x_3)\, e^{-n_2 x_3} ,$$

$$\bar{u}_3 = A_3 e^{-n_1 x_3} + (B_3 + C_3 x_3)\, e^{-n_2 x_3} , \tag{10}$$

where A_1, A_2, A_3, B_1, B_2, B_3, C_1, C_2, C_3 are independent of x_3. Substituting Equations (10) into (8) gives certain relations between these quantities as follows.

$$A_r = \frac{i\bar{x}_r}{n_1} A_3 , \quad r = 1,2 ,$$

$$B_3 = -i\left(\frac{\bar{x}_1 B_1 + \bar{x}_2 B_2}{n_2}\right) ,$$

and

$$C_j = 0 , \quad j = 1,2,3 .$$

Thus, Equation (10) can be rewritten as

$$\bar{u}_1 = \frac{i\bar{x}_1 A_3}{n_1} e^{-n_1 x_3} + B_1 e^{-n_2 x_3} ,$$

$$\bar{u}_2 = \frac{i\bar{x}_2 A_3}{n_1} e^{-n_1 x_3} + B_2 e^{-n_2 x_3} ,$$

$$\bar{u}_3 = A_3 e^{-n_1 x_3} - \frac{i}{n_2} (\bar{x}_1 B_1 + \bar{x}_2 B_2) e^{-n_2 x_3} . \qquad (11)$$

Expressions for the transformed stress components may be obtained by the substitution of Equations (11) into (5). In particular, we have

$$\bar{\sigma}_{33} = \frac{\lambda M_1^2\bar{x}_1^2 - 2\mu n_1^2}{n_1} A_3 e^{-n_1 x_3} + i2\mu(\bar{x}_1 B_1 + \bar{x}_2 B_2) e^{-n_2 x_3} ,$$

$$\bar{\sigma}_{32} = -i2\mu\bar{x}_2 A_3 e^{-n_1 x_3} - \frac{\mu}{n_2}[\bar{x}_1\bar{x}_2 B_1 + (n_2^2 + \bar{x}_2^2) B_2] e^{-n_2 x_3} ,$$

$$\bar{\sigma}_{31} = -i2\mu\bar{x}_1 A_3 e^{-n_1 x_3} - \frac{\mu}{n_2}[(n_2^2 + \bar{x}_1^2) B_1 + \bar{x}_1\bar{x}_2 B_2] e^{-n_2 x_3} . \quad (12)$$

In view of the boundary condition (7), A_3 and B_1, B_2 can be readily solved and expressed in terms of $\bar{R}_i$.

$$2\mu F A_3 = n_1[(\bar{x}_1^2 + \bar{x}_2^2 - \tfrac{1}{2} M_2^2\bar{x}_1^2) \bar{R}_3 + in_2(\bar{x}_1\bar{R}_1 + \bar{x}_2\bar{R}_2)] ,$$

$$2\mu F B_1 = -i\bar{x}_1 n_1 n_2 \bar{R}_3 + \frac{1}{n_2}\{[\bar{x}_2^2(\bar{x}_1^2 + \bar{x}_2^2 - \tfrac{1}{2} M_2^2\bar{x}_1^2 - 2n_1 n_2) + n_2^2(\bar{x}_1^2 + \bar{x}_2^2 - \tfrac{1}{2} M_2^2\bar{x}_1^2)] \bar{R}_1 - \bar{x}_1\bar{x}_2(\bar{x}_1^2 + \bar{x}_2^2 - \tfrac{1}{2} M_2^2\bar{x}_1^2 - 2n_1 n_2) \bar{R}_2\} ,$$

$$2\mu F B_2 = -i\bar{x}_2 n_1 n_2 \bar{R}_3 + \frac{1}{n_2}\{-\bar{x}_1\bar{x}_2(\bar{x}_1^2 + \bar{x}_2^2 - \tfrac{1}{2} M_2^2\bar{x}_1^2 - 2n_1 n_2) \bar{R}_1 + [\bar{x}_1^2(\bar{x}_1^2 + \bar{x}_2^2 - \tfrac{1}{2} M_2^2\bar{x}_1^2 - 2n_1 n_2) + n_2^2(\bar{x}_1^2 + \bar{x}_2^2 - \tfrac{1}{2} M_2^2\bar{x}_1^2)] \bar{R}_2\} . \quad (13)$$

Following the substitution of Equations (13) into (11), we obtain

$$2\mu F \bar{u}_1 = (i\bar{x}_1 n_3 \bar{R}_3 - \bar{x}_1^2 n_2 \bar{R}_1 - \bar{x}_1\bar{x}_2 n_2 \bar{R}_2) e^{-n_1 x_3} - \left\{ i\bar{x}_1 n_1 n_2 \bar{R}_3 - \left[\frac{\bar{x}_2^2}{n_2}(n_3 - 2n_1 n_2) + n_2 n_3\right] \bar{R}_1 + \frac{\bar{x}_1\bar{x}_2}{n_2}(n_3 - 2n_1 n_2) \bar{R}_2 \right\} e^{-n_2 x_3} ,$$

$$2\mu F\,\bar{u}_2 = (i\bar{x}_2 n_3 \bar{R}_3 - \bar{x}_1\bar{x}_2 n_2 \bar{R}_1 - \bar{x}_2^2 n_2 \bar{R}_2)\, e^{-n_1 x_3} - \Big\{ i\bar{x}_2 n_1 n_2 \bar{R}_3$$

$$+ \frac{\bar{x}_1\bar{x}_2}{n_2}(n_3 - 2n_1n_2)\,\bar{R}_1 - \left[\frac{\bar{x}_1^2}{n_2}(n_3 - 2n_1n_2) + n_2n_3\right]\bar{R}_2 \Big\} e^{-n_2 x_3} ,$$

$$2\mu F\,\bar{u}_3 = (n_1 n_3 \bar{R}_3 + i\bar{x}_1 n_1 n_2 \bar{R}_1 + i\bar{x}_2 n_1 n_2 \bar{R}_2)\, e^{-n_1 x_3}$$

$$- [n_1(\bar{x}_1^2 + \bar{x}_2^2)\,\bar{R}_3 + i\bar{x}_1 n_3 \bar{R}_1 + i\bar{x}_2 n_3 \bar{R}_2]\, e^{-n_2 x_3} , \qquad (14)$$

where

$$n_3 = \bar{x}_1^2 + \bar{x}_2^2 - \tfrac{1}{2} M_2^2 \bar{x}_1^2 , \qquad F = n_3^2 - n_1 n_2 (\bar{x}_1^2 + \bar{x}_2^2) .$$

Stress components can then be determined by the substitution of (14) into (5) in accordance with the new variables as follows

$$N_1 = n_3 - 2n_1n_2 ; \qquad N_2 = N_1/n_2 ; \qquad \bar{B} = n_3\bar{R}_3 + in_2(\bar{x}_1\bar{R}_1 + \bar{x}_2\bar{R}_2) ,$$

thus we have

$$2\mu F\,\bar{\sigma}_{11}^M = \bar{B}\,[(\bar{x}_1^2 + \bar{x}_2^2 - n_1^2)\,\lambda + 2\mu\bar{x}_1^2]\, e^{-n_1 x_3} - 2\mu\{\bar{x}_1^2 n_1 n_2 \bar{R}_3$$

$$+ i\bar{x}_1[\bar{x}_2^2 N_2 + n_2 n_3]\,\bar{R}_1 - i\bar{x}_1^2\bar{x}_2 N_2 \bar{R}_2\}\, e^{-n_2 x_3} ,$$

$$2\mu F\,\bar{\sigma}_{22}^M = \bar{B}\,[(\bar{x}_1^2 + \bar{x}_2^2 - n_1^2)\,\lambda + 2\mu\bar{x}_2^2]\, e^{-n_1 x_3} - 2\mu\{\bar{x}_2^2 n_1 n_1 \bar{R}_3$$

$$- i\bar{x}_1\bar{x}_2^2 N_2 \bar{R}_1 + i\bar{x}_2[\bar{x}_1^2 N_2 + n_2 n_3]\,\bar{R}_2\}\, e^{-n_2 x_3} ,$$

$$2\mu F\,\bar{\sigma}^{M}_{33} = \bar{B}[(\bar{x}_1^2 + \bar{x}_2^2 - n_1^2)\,\lambda - 2\mu n_1^2]\,e^{-n_1 x_3}$$

$$+ 2\mu n_2[(\bar{x}_1^2 + \bar{x}_2^2)\,n_1\bar{R}_3 + in_3(\bar{x}_1\bar{R}_1 + \bar{x}_2\bar{R}_2)]\,e^{-n_2 x_3}$$

$$2\mu F\,\bar{\sigma}^{M}_{12} = 2\mu\bar{x}_1\bar{x}_2\bar{B}\,e^{-n_1 x_3} - 2\mu\{\bar{x}_1\bar{x}_2 n_1 n_2\bar{R}_3 + \tfrac{i}{2}\,\bar{x}_2[n_2 n_3$$

$$- (\bar{x}_1^2 - \bar{x}_2^2)\,N_2]\,\bar{R}_1 + \tfrac{i}{2}\,\bar{x}_1[n_2 n_3 + (\bar{x}_1^2 - \bar{x}_2^2)\,N_2]\,\bar{R}_2\}\,e^{-n_2 x_3}\,,$$

$$2\mu F\,\bar{\sigma}^{M}_{23} = -2\mu i\bar{x}_2 n_1\bar{B}\,e^{-n_1 x_3} + \mu\{i\bar{x}_2 n_1(\bar{x}_1^2 + \bar{x}_2^2 + n_2^2)\,\bar{R}_3$$

$$- 2\bar{x}_1\bar{x}_2 n_1 n_2\bar{R}_1 - [\bar{x}_1^2 N_1 + n_3(n_2^2 + \bar{x}_2^2)]\,\bar{R}_2\}\,e^{-n_2 x_3}\,,$$

$$2\mu F\,\bar{\sigma}^{M}_{31} = -2\mu i\bar{x}_1 n_1\bar{B}\,e^{-n_1 x_3} + \mu\{i\bar{x}_1 n_1(\bar{x}_1^2 + \bar{x}_2^2 + n_2^2)\,\bar{R}_3$$

$$- [\bar{x}_2^2 N_1 + n_3(n_2^2 + \bar{x}_1^2)]\,\bar{R}_1 - 2\bar{x}_1\bar{x}_2 n_1 n_2\bar{R}_2\}\,e^{-n_2 x_3}\,. \qquad (15)$$

The displacement and stress fields are to be left in the Fourier transform expressions (14) and (15). The actual fields are to be obtained through inverse transform after the substitution of the boundary values $\{\bar{R}_i\}$.

3.0 STRESSES FROM THERMAL INPUT $\{\sigma^T_{ij}\}$

Temperature Field. The heat equation with constant thermal properties, assuming quasi-steady state and no heat generation in the medium, as expressed in terms of the convective coordinates $\{x_i\}$, is

$$\partial_{ii}T = \frac{V}{\kappa}\partial_1 T \tag{16}$$

where κ is the thermal diffusivity.

The boundary conditions at $x_3 = 0$, are

$$k\partial_3 T = \begin{cases} -q(x_1, x_2) , & \text{in the contact region} \\ 0 , & \text{elsewhere} \end{cases} \tag{17}$$

$$T,\ \partial_i T \to 0 \quad \text{as} \quad (x_i x_i)^{1/2} \to \infty . \tag{18}$$

Note that T is the temperature above the stress-free ambient, k is the thermal conductivity, q is the heat flux ($-R_1 V = \mu_f pV$), where μ_f is Coulomb coefficient and p is normal pressure distribution on the surface $x_3 = 0$. It is assumed that the mating seal, that containing the asperity, is an insulator.

The double Fourier transform of Equations (16) through (18) become, respectively,

$$[D^2 - (s^2 + in)]\,\overline{T} = 0 , \tag{19}$$

$$kD\overline{T} = \overline{Q} = \begin{cases} -\overline{q}(\overline{x}_1, \overline{x}_2) , & \text{in the contact region} \\ 0 , & \text{elsewhere} \end{cases} \tag{20}$$

$$\overline{T} \to 0 \quad \text{as} \quad x_3 \to \infty , \tag{21}$$

where $s^2 = \bar{x}_1^2 + \bar{x}_2^2$ and $n = -(V/\kappa)\,\bar{x}_1$. Now let $\bar{T} = \bar{T}_1 + i\bar{T}_2$ and $\bar{Q}/k = \bar{P}_1 + i\bar{P}_2$, then Equations (19) and (20) result in

$$(D^2 - s^2)\,\bar{T}_1 = -n\bar{T}_2 ,$$

$$(D^2 - s^2)\,\bar{T}_2 = n\bar{T}_1 \tag{22}$$

and

$$D\bar{T}_1 = \bar{P}_1 ,$$

$$D\bar{T}_2 = \bar{P}_2 \quad \text{at} \quad x_3 = 0 . \tag{23}$$

Also, (21) becomes

$$\bar{T}_1,\ \bar{T}_2 \to 0 \quad \text{as} \quad x_3 \to \infty . \tag{24}$$

Equation (22) can be expressed as a fourth-order homogeneous ordinary differential equation which is

$$[D^4 - 2s^2D^2 + (n^2 + s^4)]\,\bar{T}_r = 0 , \quad r = 1,2 . \tag{25}$$

In view of the regularity condition (24), the solution of Equation (25) has the form

$$\bar{T}_r = e^{-\omega z}[A_r \cos \theta z + B_r \sin \theta z] \tag{26}$$

where

$$\theta = \left[\frac{(s^4 + n^2)^{1/2} - s^2}{2}\right]^{1/2} ,$$

$$\omega = \left[\frac{(s^4 + n^2)^{1/2} + s^2}{2}\right]^{1/2} .$$

Substituting (26) into (22) and (23) gives

$$\bar{P}_r = -\omega A_r + \theta B_r , \quad r = 1,2 \tag{27}$$

and

$$A_1 = -\frac{n}{2\omega\theta} B_2 , \tag{28}$$

$$B_1 = \frac{n}{2\omega\theta} A_2 . \tag{29}$$

Hence, we have four equations for four unknowns A_1, A_2, B_1 and B_2, which can be readily obtained.

$$A_1 = -\frac{2\omega^2\bar{P}_1 + n\bar{P}_2}{2\omega(\omega^2 + \theta^2)} ,$$

$$A_2 = \frac{n\bar{P}_1 - 2\omega^2\bar{P}_2}{2\omega(\omega^2 + \theta^2)} ,$$

$$B_1 = \frac{2\theta^2\bar{P}_1 - n\bar{P}_2}{2\theta(\omega^2 + \theta^2)} ,$$

$$B_2 = \frac{n\bar{P}_1 + 2\theta^2\bar{P}_2}{2\theta(\omega^2 + \theta^2)} . \tag{30}$$

Following the substitution of the expression (30) into (26) and according to $\bar{T} = \bar{T}_1 + i\bar{T}_2$, we obtain $\bar{T}$ as

$$\bar{T} = e^{-\omega x_3} [(C_1 \cos \theta x_3 + C_2 \sin \theta x_3) \bar{P}_1 + (C_3 \cos \theta x_3 + C_4 \sin \theta x_3) \bar{P}_2] , \quad (31)$$

where

$$C_1 = \frac{-2\omega^2 + in}{2\omega(\omega^2 + \theta^2)} ,$$

$$C_2 = \frac{2\theta^2 + in}{2\theta(\omega^2 + \theta^2)} ,$$

$$C_3 = \frac{-n - i2\omega^2}{2\omega(\omega^2 + \theta^2)} ,$$

$$C_4 = \frac{-n + i2\theta^2}{2\theta(\omega^2 + \theta^2)} ,$$

Again, the temperature field is left in the Fourier transformed expression, which will be used in solving the thermal stress field. To be complete and also for comparison, the Green's function solution approach for the temperature field is given in the following.

The Green's function solution can be expressed as

$$g(x_1 - x_1', x_2 - x_2', x_3, t - t') = \frac{dt'}{4\rho C[\pi\kappa(t - t')]^{3/2}} \cdot \exp\left\{ - \frac{[(x_1 - x_1') - V(t - t')]^2 + (x_2 - x_2')^2 + x_3^2}{4\kappa(t - t')} \right\} \quad (32)$$

which is the temperature at time t at the location (x_1, x_2, x_3) due to the unit heat flux input emitted at time t' at the location $(x_1', x_2', 0)$. It can be easily shown that Equation (32) satisfies the governing heat equation (16).

The temperature field can be obtained by the convolution integral as

$$T(x_1,x_2,x_3,t) = \int_{B_H} q(x_1',x_2')\, K_o(x_1 - x_1', x_2 - x_2', x_3, t - t')\, dx_1'\, dx_2' \tag{33}$$

where B_H indicates the heat-flux input region and

$$K_o = \int_o^t g(x_1 - x_1', x_2 - x_2', x_3, t - t')\, dt' \ . \tag{34}$$

Substituting (32) into (34) and changing the variable by letting $\tau = R/2\sqrt{\kappa(t - t')}$, K_o becomes

$$K_o = \frac{e^{V(x_1-x_1')/2\kappa}}{\pi^{3/2}\, kR} \int_{R/2\sqrt{\kappa t}}^{\infty} e^{-\tau^2-(V^2R^2/16\kappa^2\tau^2)}\, d\tau \tag{35}$$

where ρ = density

c = specific heat

$k = \rho c \kappa$

$R = [(x_1 - x_1')^2 + (x_2 - x_2')^2 + x_3^2]^{1/2}$.

Considering the steady-state solution, i.e., $t \to \infty$, Equation (35) results in

$$G(x_1 - x_1', x_2 - x_2', x_3) = \lim_{t \to \infty} K_o$$

$$= \frac{1}{2\pi kR} e^{-V[R - (x_1 - x_1')]/2\kappa} . \qquad (36)$$

Accordingly, the steady-state temperature field can be obtained as

$$T(x_1,x_2,x_3) = \frac{1}{2\pi k} \int_{B_H} q(x_1',x_2') \frac{e^{-V[R-(x_1-x_1')]/2\kappa}}{R} dx_1' dx_2' \qquad (37)$$

which will be employed to give the numerical results for different cases of application.

Thermal Stress Field. The governing equations for the thermal stress solutions are based on the theory of quasi-static uncoupled thermoelasticity. The governing equations are then

$$\mu \nabla^2 u_j + (\lambda + \mu) \partial_j (\nabla \cdot \underset{\sim}{u}) = (3\lambda + 2\mu) \alpha \partial_j T \qquad (38)$$

and

$$\sigma_{ij}^T = \lambda \partial_k u_k \delta_{ij} + \mu(\partial_j u_i + \partial_i u_j) - (3\lambda + 2\mu) \alpha T \delta_{ij} \qquad (39)$$

subject to the boundary conditions

$$\sigma_{3i}^T = 0 , \quad i = 1,2,3 \quad \text{at} \quad x_3 = 0 , \qquad (40)$$

$$\sigma_{ij}^T , \; u_i \to 0 \quad \text{as} \quad (x_i x_i)^{1/2} \to \infty . \qquad (41)$$

The double Fourier transforms of Equations (38) through (41) are

$$[D^2 - (a_1\bar{x}_1^2 + \bar{x}_2^2)]\,\bar{u}_1 - a_2\bar{x}_1\bar{x}_2\bar{u}_2 - ia_2\bar{x}_1 D\bar{u}_3 = -ia_3\bar{x}_1\bar{T}\,, \tag{42}$$

$$-a_2\bar{x}_1\bar{x}_2\bar{u}_1[D^2 - (a_1\bar{x}_2^2 + \bar{x}_1^2)]\,\bar{u}_2 - ia_2\bar{x}_2 D\bar{u}_3 = -ia_3\bar{x}_2\bar{T}\,, \tag{43}$$

$$-ia_2\bar{x}_1 D\bar{u}_1 - ia_2\bar{x}_2 D\bar{u}_2 + (a_1 D^2 - s^2)\,\bar{u}_3 = a_3 D\bar{T}\,, \tag{44}$$

$$\frac{\bar{\sigma}_{11}^T}{\mu} = -i(a_1\bar{x}_1\bar{u}_1 + r\bar{x}_2\bar{u}_2) + rD\bar{u}_3 - a_3\bar{T}\,, \tag{45}$$

$$\frac{\bar{\sigma}_{22}^T}{\mu} = -i(r\bar{x}_1\bar{u}_1 + a_1\bar{x}_2\bar{u}_2) + rD\bar{u}_3 - a_3\bar{T}\,, \tag{46}$$

$$\frac{\bar{\sigma}_{33}^T}{\mu} = -ir(\bar{x}_1\bar{u}_1 + \bar{x}_2\bar{u}_2) + a_1 D\bar{u}_3 - a_3\bar{T}\,, \tag{47}$$

$$\frac{\bar{\sigma}_{12}^T}{\mu} = -i(\bar{x}_2\bar{u}_1 + \bar{x}_1\bar{u}_2)\,, \tag{48}$$

$$\frac{\bar{\sigma}_{23}^T}{\mu} = D\bar{u}_2 - i\bar{x}_2\bar{u}_3\,, \tag{49}$$

$$\frac{\bar{\sigma}_{31}^T}{\mu} = D\bar{u}_1 - i\bar{x}_1\bar{u}_3\,, \tag{50}$$

$$\bar{\sigma}_{3i}^T = 0\,, \qquad i = 1,2,3 \quad \text{at} \quad x_3 = 0\,, \tag{51}$$

$$\bar{\sigma}_{ij}^T\,, \qquad \bar{u}_i \to 0 \quad \text{as} \quad (\bar{x}_i\bar{x}_i)^{1/2} \to \infty\,, \tag{52}$$

where $r = \lambda/\mu$, $a_1 = r + 2$, $a_2 = r + 1$ and $a_3 = (3r + 2)\,\alpha$.

Equations (42) through (44) form a system of three simultaneous linear differential equations. The dependent variables $\bar{u}_i$ are to be solved. The system can be rewritten as

$$\Delta \bar{u}_i = \Delta_i \ , \quad i = 1,2,3 \tag{53}$$

where Δ is a differential operator that is the determinant of the system,

$$\Delta = \begin{vmatrix} D^2 - (a_1\bar{x}_1 + \bar{x}_2^2) & -a_2\bar{x}_1\bar{x}_2 & -ia_2\bar{x}_1 D \\ -a_2\bar{x}_1\bar{x}_2 & D^2 - (a_1\bar{x}_2^2 + \bar{x}_1^2) & -ia_2\bar{x}_2 D \\ -ia_2\bar{x}_1 D & -ia_2\bar{x}_2 D & a_1 D^2 - s^2 \end{vmatrix}$$

$$= a_1(D^2 - s^2)^3 \tag{54}$$

and Δ_i's are

$$\Delta_1 = \begin{vmatrix} -ia_3\bar{x}_1\bar{T} & -a_2\bar{x}_1\bar{x}_2 & -ia_2\bar{x}_1 D \\ -ia_3\bar{x}_2\bar{T} & D^2 - (a_1\bar{x}_2^2 + \bar{x}_1^2) & -ia_2\bar{x}_2 D \\ a_3 D\bar{T} & -ia_2\bar{x}_2 D & a_1 D^2 - s^2 \end{vmatrix},$$

$$\Delta_2 = \begin{vmatrix} D^2 - (a_1\bar{x}_1^2 + \bar{x}_2^2) & -ia_3\bar{x}_1\bar{T} & -ia_2\bar{x}_1 D \\ -a_2\bar{x}_1\bar{x}_2 & -ia_3\bar{x}_2\bar{T} & -ia_2\bar{x}_2 D \\ -ia_2\bar{x}_1 D & a_3 D\bar{T} & a_1 D^2 - s^2 \end{vmatrix},$$

$$\Delta_3 = \begin{vmatrix} D^2 - (a_1\bar{x}_1^2 + \bar{x}_2^2) & -a_2\bar{x}_1\bar{x}_2 & -ia_3\bar{x}_1\bar{T} \\ -a_2\bar{x}_1\bar{x}_2 & D^2 - (a_1\bar{x}_2^2 + \bar{x}_1^2) & -ia_3\bar{x}_2\bar{T} \\ -ia_2\bar{x}_1 D & -ia_2\bar{x}_2 D & a_3 D\bar{T} \end{vmatrix} ,$$

The solutions obtained through Equation (53) are particular solutions which are

$$\bar{u}_r^p = \frac{a_3\bar{x}_r}{2a_1\omega\theta}(G_r \cos \theta x_3 + H_r \sin \theta x_3)\, e^{-\omega x_3} , \quad r = 1,2 ,$$

$$\bar{u}_3^p = \frac{a_3}{2a_1\omega\theta}(G_3 \cos \theta x_3 + H_3 \sin \theta x_3)\, e^{-\omega x_3} \tag{55}$$

where

$$G_1 = G_2 = B_2 - iB_1 , \quad H_1 = H_2 = -A_2 + iA_1 ,$$

$$G_3 = -i(\omega G_1 - \theta H_1) , \quad H_3 = -i(\omega H_1 - \theta G_1) .$$

A_1, A_2, B_1 and B_2 are shown in Equation (30). The complementary solutions can be determined by $\Delta u_i = 0$. In view of Equation (54) and considering the regularity condition, we obtain

$$\bar{u}_1^c = \frac{\bar{x}_1}{\bar{x}_2}(h_1 + h_2 x_3)\, e^{-sx_3} ,$$

$$\bar{u}_2^c = (h_1 + h_2 x_3)\, e^{-sx_3} ,$$

$$\bar{u}_3^c = -\frac{i}{a_2\bar{x}_2}\left[a_2 s(h_1 + h_2 x_3) + (a_2 + 2)\, h_2\right] e^{-sx_3} . \tag{56}$$

With regard to Equations (55) and (56), the general solutions are

$$\bar{u}_i = \bar{u}_i^p + \bar{u}_i^c , \quad i = 1,2,3 . \tag{57}$$

Two unknowns h_1 and h_2 will be determined by substituting Equation (57) into Equations (47) and (49) and employing the boundary condition (51), thus we have

$$h_1 = \frac{a_3\bar{x}_2}{2a_1 a_2 s^2\omega\theta}\left[a_1 s\theta\, H_1 + (s^2 - a_1 s\omega + a_1\theta^2)\, G_1\right] ,$$

$$h_2 = \frac{a_3\bar{x}_2}{2a_1 s\omega\theta}\left[-s\theta\, H_1 - (s^2 - s\omega + a_1\theta^2)\, G_1\right] . \tag{58}$$

Following the substitution of the displacement solution, (56) through (58), into Equations (45) through (50), the thermal stress field can be readily obtained.

$$\frac{\bar{\sigma}_{11}^T}{\mu} = i\left[(-b_1 H_1 + b_2 G_1)\, e^{-\omega x_3} + (-b_3 H_1 + b_4 G_1)\, e^{-sx_3}\right] ,$$

$$\frac{\bar{\sigma}_{22}^T}{\mu} = i\left[(-b_5 H_1 + b_6 G_1)\, e^{-\omega x_3} + (-b_7 H_1 + b_8 G_1)\, e^{-sx_3}\right] ,$$

$$\frac{\bar{\sigma}_{33}^T}{\mu} = i\left[(-b_9 H_1 + b_{10} G_1)\, e^{-\omega x_3} + (b_{11} H_1 - b_{12} G_1)\, e^{-sx_3}\right] ,$$

$$\frac{\bar{\sigma}_{12}^T}{\mu} = i\left[(-b_{13}H_1 + b_{14}G_1)\, e^{-\omega x_3} + (-b_{15}H_1 + b_{16}G_1)\, \bar{x}_1\bar{x}_2\, e^{-sx_3}\right],$$

$$\frac{\bar{\sigma}_{23}^T}{\mu} = -\bar{x}_2\left[(b_{17}H_1 - b_{18}G_1)\, e^{-\omega x_3} - (b_{19}H_1 - b_{20}G_1)\, e^{-sx_3}\right],$$

$$\frac{\bar{\sigma}_{31}^T}{\mu} = -\bar{x}_1\left[(b_{17}H_1 - b_{18}G_1)\, e^{-\omega x_3} - (b_{19}H_1 - b_{20}G_1)\, e^{-sx_3}\right], \qquad (59)$$

where

$$H_1 = \frac{-(n + i2\omega^2)\,\bar{P}_1 + (2\omega^2 - in)\,\bar{P}_2}{2\omega(\omega^2 + \theta^2)} = i(C_1\bar{P}_1 + C_3\bar{P}_2),$$

$$G_1 = \frac{(n - i2\theta^2)\,\bar{P}_1 + (2\theta^2 + in)\,\bar{P}_2}{2\theta(\omega^2 + \theta^2)} = -i(C_2\bar{P}_1 + C_4\bar{P}_2),$$

$$b_1 = \frac{-a_3}{a_1\omega\theta}\,(2\omega\theta\cos\theta x_3 - \bar{x}_1^2\sin\theta x_3),$$

$$b_2 = \frac{-a_3}{a_1\omega\theta}\,(\bar{x}_1^2\cos\theta x_3 + 2\omega\theta\sin\theta x_3),$$

$$b_3 = \frac{a_3}{\omega}\left(\frac{\bar{x}_1^2}{a_2 s} + \frac{rs}{a_1 a_2} - \frac{\bar{x}_1^2 x_3}{a_1}\right),$$

$$b_4 = \frac{a_3}{a_1\omega\theta}\left[\frac{a_1\omega - s}{a_2 s}\,\bar{x}_1^2 + \frac{r(s\omega - s^2)}{a_2} + (s - \omega)\,\bar{x}_1^2 x_3\right],$$

$$b_5 = \frac{-a_3}{a_1\omega\theta}\,(2\omega\theta\cos\theta x_3 - \bar{x}_2^2\sin\theta x_3),$$

$$b_6 = \frac{-a_3}{a_1\omega\theta}\left(\bar{x}_2^2 \cos \theta x_3 + 2\omega\theta \sin \theta x_3\right),$$

$$b_7 = \frac{a_3}{\omega}\left(\frac{\bar{x}_2^2}{a_2 s} + \frac{rs}{a_1 a_2} - \frac{\bar{x}_2^2 x_3}{a_1}\right),$$

$$b_8 = \frac{a_3}{a_1\omega\theta}\left[\frac{a_1\omega - s}{a_2 s}\bar{x}_2^2 + \frac{r(s\omega - s^2)}{a_2} + (s - \omega)\bar{x}_2^2 x_3\right],$$

$$b_9 = \frac{-a_3 s^2}{a_1\omega\theta} \sin \theta x_3 ,$$

$$b_{10} = \frac{a_3 s^2}{a_1\omega\theta} \cos \theta x_3 ,$$

$$b_{11} = -\frac{a_3 s^2}{a_1\omega} x_3 ,$$

$$b_{12} = \frac{a_3 s^2}{a_1\omega\theta}\left[1 + (s - \omega) x_3\right],$$

$$b_{13} = \frac{a_3\bar{x}_1\bar{x}_2}{a_1\omega\theta} \sin \theta x_3 ,$$

$$b_{14} = -\frac{a_3\bar{x}_1\bar{x}_2}{a_1\omega\theta} \cos \theta x_3 ,$$

$$b_{15} = \frac{a_3}{\omega}\left(\frac{1}{a_2 s} - \frac{x_3}{a_1}\right),$$

$$b_{16} = \frac{a_3}{a_1\omega\theta}\left[\frac{a_1\omega - s}{a_2 s} + (s - \omega)\, x_3\right],$$

$$b_{17} = \frac{a_3}{a_1\omega\theta}\,(-\theta \cos \theta x_3 + \omega \sin \theta x_3),$$

$$b_{18} = \frac{-a_3}{a_1\omega\theta}\,(\omega \cos \theta x_3 + \theta \sin \theta x_3),$$

$$b_{19} = \frac{a_3}{a_1\omega}\,(-1 + s x_3),$$

$$b_{20} = \frac{a_3}{a_1\omega\theta}\,[-\omega + s(\omega - s)\, x_3],$$

Note that $\overline{P}_1$ and $\overline{P}_2$ are the real and imaginary part of $\overline{Q}/k$. Therefore

$$\overline{P}_1 = \frac{1}{2\pi k}\int_{B_H} Q(x_1, x_2) \cos\,(\overline{x}_1 x_1 + \overline{x}_2 x_2)\, dx_1\, dx_2,$$

$$\overline{P}_2 = \frac{1}{2\pi k}\int_{B_H} Q(x_1, x_2) \sin\,(\overline{x}_1 x_1 + \overline{x}_2 x_2)\, dx_1\, dx_2. \qquad (60)$$

For the case $\overline{P}_2 = 0$, Equations (59) become

$$\frac{\overline{\sigma}^T_{11}}{\mu} = \overline{P}_1\left[(b_1C_1 + b_2C_2)\, e^{-\omega x_3} + (b_3C_1 + b_4C_2)\, e^{-s x_3}\right],$$

$$\frac{\overline{\sigma}^T_{22}}{\mu} = \overline{P}_1\left[(b_5C_1 + b_6C_2)\, e^{-\omega x_3} + (b_7C_1 + b_8C_2)\, e^{-s x_3}\right],$$

$$\frac{\bar{\sigma}^I_{33}}{\mu} = \bar{P}_1\left[(b_9C_1 + b_{10}C_2)\, e^{-\omega x_3} - (b_{11}C_1 + b_{12}C_2)\, e^{-sx_3}\right],$$

$$\frac{\bar{\sigma}^I_{12}}{\mu} = \bar{P}_1\left[(b_{13}C_1 + b_{14}C_2)\, e^{-\omega x_3} + (b_{15}C_1 + b_{16}C_2)\, \bar{x}_1\bar{x}_2\, e^{-sx_3}\right],$$

$$\frac{\bar{\sigma}^I_{23}}{\mu} = -i\bar{x}_2\bar{P}_1\left[(b_{17}C_1 + b_{18}C_2)\, e^{-\omega x_3} - (b_{19}C_1 + b_{20}C_2)\, e^{-sx_3}\right],$$

$$\frac{\bar{\sigma}^I_{31}}{\mu} = -i\bar{x}_1\bar{P}_1\left[(b_{17}C_1 + b_{18}C_2)\, e^{-\omega x_3} - (b_{19}C_1 + b_{20}C_2)\, e^{-sx_3}\right]. \quad (61)$$

4.0 NUMERICAL RESULTS

Previous sections have shown the general expressions for the transformed mechanical and thermal stress fields. Applying the inverse Fourier transform and following through the simplification of the multiple integrals, results for several cases can be obtained numerically.

4.1 A Moving Rectangular Contact Area of Uniform Pressure (Case 1)

Mechanical Stress Field

The tractions of the mechanical loading are

$$\sigma_{33} = -R_3(x_1, x_2, 0) , \quad \sigma_{32} = -R_2 = 0 , \quad \sigma_{31} = -R_1(x_1, x_2, 0)$$

where

$$R_3 = \begin{cases} p_o = \text{constant} , & x_1 \leq a, \ x_2 \leq b \\ 0 , & \text{elsewhere} \end{cases}$$

$$R_1 = -\mu_f R_3 .$$

The corresponding transformed boundary conditions can be readily obtained

$$\bar{R}_3(\bar{x}_1, \bar{x}_2, 0) = \frac{1}{2\pi} \int_{-\infty}^{\infty} \int_{-\infty}^{\infty} R_3 \, e^{i(\bar{x}_1 x_1 + \bar{x}_2 x_2)} \, dx_1 \, dx_2$$

$$= \frac{1}{2\pi} \int_{-b}^{b} \int_{-a}^{a} p_o \, e^{i(\bar{x}_1 x_1 + \bar{x}_2 x_2)} \, dx_1 \, dx_2$$

$$= \frac{p_o}{2\pi} \left[\int_{-b}^{b} e^{i\bar{x}_2 x_2} \, dx_2 \right] \left[\int_{-a}^{a} e^{i\bar{x}_1 x_1} \, dx_1 \right]$$

(Equation continued on next page.)

$$= \frac{2P_o}{\pi \bar{x}_1 \bar{x}_2} \sin(\bar{x}_1 a) \sin(\bar{x}_2 b) ,$$

$$\bar{R}_1 = -\mu_f \bar{R}_3 , \quad \bar{R}_2 = 0 . \tag{62}$$

Following the substitution of (62) into (15) and applying the inverse transform, the mechanical stress components can be expressed as

$$\{\sigma_{ij}\} = \{\sigma^n_{ij}\} + \{\sigma^f_{ij}\}$$

where the first term on the right-hand side of this equation denotes the stress components resulting from the normal loading $\bar{R}_3$, and the second the frictional loading $\bar{R}_1$. The expressions are

$$\sigma^n_{11} = \frac{P_o}{\pi^2} \int_0^{2\pi} \frac{\cot \phi}{H} \int_0^{\infty} \left[\gamma_3 (1 + \frac{1}{2} M_2^2 - M_1^2) \, e^{-s\gamma_1 x_3} - \gamma_1 \gamma_2 \, e^{-s\gamma_2 x_3} \right] \cdot W(s,\phi) \, ds \, d\phi ,$$

$$\sigma^n_{22} = \frac{P_o}{\pi^2} \int_0^{2\pi} \frac{1}{H \sin \phi \cos \phi} \int_0^{\infty} \left\{ [\gamma_3 (\frac{1}{2} \beta^2 - 1) \, M_1^2 \cos^2 \phi + \sin^2 \phi] \cdot e^{-s\gamma_1 x_3} - \gamma_1 \gamma_2 \sin^2 \phi \, e^{-s\gamma_2 x_3} \right\} W(s,\phi) \, ds \, d\phi ,$$

$$\sigma^n_{33} = \frac{-P_o}{\pi^2} \int_0^{2\pi} \frac{1}{H \sin \phi \cos \phi} \int_0^{\infty} \left[\gamma_3^2 \, e^{-s\gamma_1 x_3} - \gamma_1 \gamma_2 \, e^{-s\gamma_2 x_3} \right] \cdot W(s,\phi) \, ds \, d\phi ,$$

$$\sigma^n_{12} = \frac{P_o}{\pi^2} \int_0^{2\pi} \frac{1}{H} \int_0^{\infty} \left[\gamma_3 \, e^{-s\gamma_1 x_3} - \gamma_1 \gamma_2 \, e^{-s\gamma_2 x_3} \right] W(s,\phi) \, ds \, d\phi ,$$

$$\sigma_{23}^{n} = \frac{-iP_o}{\pi^2} \int_0^{2\pi} \frac{\gamma_1\gamma_3}{H \cos\phi} \int_0^{\infty} \left[e^{-s\gamma_1 x_3} - e^{-s\gamma_2 x_3} \right] W(s,\phi)\, ds\, d\phi ,$$

$$\sigma_{31}^{n} = \frac{-iP_o}{\pi^2} \int_0^{2\pi} \frac{\gamma_1\gamma_3}{H \sin\phi} \int_0^{\infty} \left[e^{-s\gamma_1 x_3} - e^{-s\gamma_2 x_3} \right] W(s,\phi)\, ds\, d\phi ,$$

$$\sigma_{11}^{f} = \frac{-i\mu_f P_o}{\pi^2} \int_0^{2\pi} \frac{1}{H \sin\phi} \int_0^{\infty} \left\{ \gamma_2 \cos^2\phi \left(1 + \tfrac{1}{2} M_2^2 - M_1^2\right) e^{-s\gamma_1 x_3} - \left[\frac{(\gamma_3 - 2\gamma_1\gamma_2)}{\gamma_2} \sin^2\phi + \gamma_2\gamma_3 \right] e^{-s\gamma_2 x_3} \right\} W(s,\phi)\, ds\, d\phi ,$$

$$\sigma_{22}^{f} = \frac{-i\mu_f P_o}{\pi^2} \int_0^{2\pi} \frac{1}{H \sin\phi} \int_0^{\infty} \left\{ \gamma_2 \left[\left(\tfrac{1}{2}\beta^2 - 1\right) M_1^2 \cos^2\phi + \sin^2\phi \right] e^{-s\gamma_1 x_3} + \left[\frac{(\gamma_3 - 2\gamma_1\gamma_2)}{\gamma_2} \sin^2\phi \right] e^{-s\gamma_2 x_3} \right\} W(s,\phi)\, ds\, d\phi ,$$

$$\sigma_{33}^{f} = \frac{-i\mu_f P_o}{\pi^2} \int_0^{2\pi} \frac{\gamma_2}{H \sin\phi} \int_0^{\infty} \left\{ \left[\left(\tfrac{1}{2}\beta^2 - 1\right) M_1^2 \cos^2\phi - \gamma_1^2 \right] e^{-s\gamma_1 x_3} + \gamma_3\, e^{-s\gamma_2 x_3} \right\} W(s,\phi)\, ds\, d\phi ,$$

$$\sigma_{12}^{f} = \frac{-i\mu_f P_o}{\pi^2} \int_0^{2\pi} \frac{\gamma_2}{H \cos\phi} \int_0^{\infty} \left\{ \cos^2\phi\, e^{-s\gamma_1 x_3} - \tfrac{1}{2} \left[\frac{(\gamma_3 - 2\gamma_1\gamma_2)}{\gamma_2^2} \cdot (\sin^2\phi - \cos^2\phi) + \gamma_3 \right] e^{-s\gamma_2 x_3} \right\} W(s,\phi)\, ds\, d\phi ,$$

$$\sigma_{23}^f = \frac{-\mu_f P_0}{\pi^2} \int_0^{2\pi} \frac{\gamma_1 \gamma_2}{H} \int_0^{\infty} \left(e^{-s\gamma_1 x_3} - e^{-s\gamma_2 x_3} \right) W(s,\phi)\, ds\, d\phi ,$$

$$\sigma_{31}^f = \frac{-\mu_f P_0}{\pi^2} \int_0^{2\pi} \frac{1}{H \sin\phi \cos\phi} \int_0^{\infty} \left[\gamma_1 \gamma_2 \cos^2\phi\, e^{-s\gamma_1 x_3} - (\gamma_3^2 - \gamma_1 \gamma_2 \sin^2\phi)\, e^{-s\gamma_2 x_3} \right] W(s,\phi)\, ds\, d\phi , \tag{63}$$

where

$$W(s,\phi) = \frac{\sin(sa\cos\phi)\,\sin(sb\sin\phi)}{s} e^{-is\gamma\cos(\theta-\phi)} ,$$

$$\gamma = (x_1^2 + x_2^2)^{1/2} , \qquad \gamma_3 = (1 - \tfrac{1}{2} M_2^2 \cos^2\phi) ,$$

$$\gamma_t = (1 - M_t^2 \cos^2\phi)^{1/2} , \qquad t = 1,2 ,$$

$$H = \gamma_3^2 - \gamma_1\gamma_2 , \qquad \theta = \tan^{-1}\frac{x_2}{x_1} .$$

Equations (63) can be reduced to single integrals by using the techniques of change of variables and the following equalities:

$$\frac{\sin(sa\cos\phi)\,\sin(sb\sin\phi)}{s} e^{-s\gamma_t x_3} \cos(s\gamma\cos(\theta-\phi))$$

$$= \frac{1}{4}\frac{1}{s} e^{-s\gamma_t x_3} \{[\cos s(a\cos\phi - b\sin\phi - \gamma\cos(\theta-\phi)) + \cos s(a\cos\phi - b\sin\phi + \gamma\cos(\theta-\phi))] - [\cos s(a\cos\phi + b\sin\phi - \gamma\cos(\theta-\phi)) + \cos s(a\cos\phi + b\sin\phi + \gamma\cos(\theta-\phi))]\} ,$$

$$\frac{\sin(sa\cos\phi)\,\sin(sb\sin\phi)}{s}\,e^{-s\gamma_t x_3}\,\sin(s\,\gamma\cos(\theta-\phi))$$

$$= \frac{1}{4}\frac{1}{s}\,e^{-s\gamma_t x_3}\,\{[\sin s(a\cos\phi - b\sin\phi + \gamma\cos(\theta-\phi)) - \sin s(a\cos\phi - b\sin\phi - \gamma\cos(\theta-\phi))] - [\sin s(a\cos\phi + b\sin\phi + \gamma\cos(\theta-\phi)) - \sin s(a\cos\phi + b\sin\phi - \gamma\cos(\theta-\phi))]\}\,,$$

$$\int_0^\infty \frac{1}{s}\,e^{-sd}\,\sin(se)\,ds = \tan^{-1}\left(\frac{e}{d}\right)\,,$$

$$\int_0^\infty \frac{1}{s}\,e^{-sd}\,\cos(se)\,ds = \int_0^\infty \frac{1}{s}\,e^{-sd}\,ds - \frac{1}{2}\ln\left(\frac{e^2+d^2}{d^2}\right)\,.$$

The term $\int_0^\infty \frac{1}{s}\,e^{-sd}\,ds$ cancels out during simplification. Thus, the stress fields are expressed as

$$\sigma_{11}^n = \frac{P_0}{4\pi^2}\int_0^\pi \frac{\cot\phi}{H}\,[\gamma_3(1+\tfrac{1}{2}M_2^2 - M_1^2)\,S_1 - \gamma_1\gamma_2 S_2]\,d\phi\,,$$

$$\sigma_{22}^n = \frac{P_0}{2\pi^2}\int_0^\pi \frac{1}{H\sin 2\phi}\,\{[\gamma_3(\tfrac{1}{2}\beta^2 - 1)\,M_1^2\cos^2\phi + \sin^2\phi] \cdot S_1 - \gamma_1\gamma_2\sin^2\phi\,S_2\}\,d\phi\,,$$

$$\sigma_{33}^n = \frac{-P_0}{2\pi^2}\int_0^\pi \frac{1}{H\sin 2\phi}\,[\gamma_3^2 S_1 - \gamma_1\gamma_2 S_2]\,d\phi\,,$$

$$\sigma_{12}^n = \frac{P_0}{4\pi^2}\int_0^\pi \frac{1}{H}\,[\gamma_3 S_1 - \gamma_1\gamma_2 S_2]\,d\phi\,,$$

$$\sigma_{23}^{n} = \frac{-P_o}{2\pi^2} \int_0^{\pi} \frac{\gamma_1 \gamma_3}{H \cos \phi} [W_1 - W_2] \, d\phi \, ,$$

$$\sigma_{31}^{n} = \frac{-P_o}{2\pi^2} \int_0^{\pi} \frac{\gamma_1 \gamma_3}{H \sin \phi} [W_1 - W_2] \, d\phi \, ,$$

$$\sigma_{11}^{f} = \frac{-\mu_f P_o}{2\pi^2} \int_0^{\pi} \frac{1}{H \sin \phi} \left\{ \gamma_2 \cos^2 \phi (1 + \tfrac{1}{2} M_2^2 - M_1^2) \, W_1 - \left[\frac{(\gamma_3 - 2\gamma_1\gamma_2)}{\gamma^2} \sin^2 \phi + \gamma_2 \gamma_3 \right] W_2 \right\} d\phi \, ,$$

$$\sigma_{22}^{f} = \frac{-\mu_f P_o}{2\pi^2} \int_0^{\pi} \frac{1}{H \sin \phi} \left\{ \gamma_2 [(\tfrac{1}{2} \beta^2 - 1) M_1^2 \cos^2 \phi + \sin^2 \phi] \, W_1 + \left[\frac{(\gamma_3 - 2\gamma_1\gamma_2)}{\gamma_2} \sin^2 \phi \right] W_2 \right\} d\phi \, ,$$

$$\sigma_{33}^{f} = \frac{-\mu_f P_o}{2\pi^2} \int_0^{\pi} \frac{\gamma_2}{H \sin \phi} \{ [(\tfrac{1}{2} \beta^2 - 1) M_1^2 \cos^2 \phi - \gamma_1^2] \, W_1 + \gamma_3 W_2 \} \, d\phi \, ,$$

$$\sigma_{12}^{f} = \frac{-\mu_f P_o}{2\pi^2} \int_0^{\pi} \frac{\gamma_2}{H \cos \phi} \left\{ \cos^2 \phi \, W_1 - \frac{1}{2} \left[\frac{(\gamma_3 - 2\gamma_1\gamma_2)}{\gamma_2^2} \cdot (\sin^2 \phi - \cos^2 \phi) + \gamma_3 \right] W_2 \right\} d\phi \, ,$$

$$\sigma_{23}^{f} = \frac{-\mu_f P_o}{4\pi^2} \int_0^{\pi} \frac{\gamma_1 \gamma_2}{H} [S_1 - S_2] \, d\phi \, ,$$

$$\sigma_{31}^{f} = \frac{-\mu_f P_o}{2\pi^2} \int_0^{\pi} \frac{1}{H \sin^2 \phi} [\gamma_1 \gamma_2 \cos^2 \phi \, S_1 - (\gamma_3^2 - \gamma_1 \gamma_2 \sin^2 \phi) \, S_2] \, d\phi \tag{64}$$

in which

$$S_t = \ln \frac{\{[a \cos \phi + b \sin \phi + \gamma \cos(\theta - \phi)]^2 + \gamma_t^2 x_3^2\}}{\{[a \cos \phi - b \sin \phi - \gamma \cos(\theta - \phi)]^2 + \gamma_t^2 x_3^2\}}$$

$$+ \ln \frac{\{[a \cos \phi + b \sin \phi - \gamma \cos(\theta - \phi)]^2 + \gamma_t^2 x_3^2\}}{\{[a \cos \phi - b \sin \phi + \gamma \cos(\theta - \phi)]^2 + \gamma_t^2 x_3^2\}}$$

$$W_t = \tan^{-1} \frac{a \cos \phi - b \sin \phi + \gamma \cos(\theta - \phi)}{\gamma_t x_3}$$

$$+ \tan^{-1} \frac{a \cos \phi + b \sin \phi - \gamma \cos(\theta - \phi)}{\gamma_t x_3}$$

$$- \tan^{-1} \frac{a \cos \phi - b \sin \phi - \gamma \cos(\theta - \phi)}{\gamma_t x_3}$$

$$- \tan^{-1} \frac{a \cos \phi + b \sin \phi + \gamma \cos(\theta - \phi)}{\gamma_t x_3}$$

$$t = 1,2 \; .$$

The integrals appearing in Equations (64) are suitable for numerical evaluation at any point inside the solid. However, most integrals are not defined at $\phi = 0$, $\pi/2$ or π. Limiting processes are imperative so that singularities can be removed.

Thermal Stress Field

Replacing $Q(x_1,x_2)$ in (60) by expressions (20) and (17), we obtain

$$\overline{P}_1 = \frac{-1}{2\pi k} \int_{B_H} q(x_1, x_2) \cos(\overline{x}_1\overline{x}_1 + \overline{x}_2 x_2)\, dx_1\, dx_2$$

$$= \frac{-\mu_f P_o V}{2\pi k} \int_{-a}^{a} \int_{-b}^{b} \cos(\overline{x}_1 x + \overline{x}_2 x)\, dx_2\, dx_1$$

$$= \frac{-\mu_f P_o V}{\pi k} \cdot \frac{\sin(\overline{x}_2 b)}{\overline{x}_2} \int_{-a}^{a} \cos(\overline{x}_1 x)\, dx_1$$

$$= \frac{-2\mu_f P_o V}{\pi k} \cdot \frac{1}{\overline{x}_1\overline{x}_2} \sin(\overline{x}_1 a) \sin(\overline{x}_2 b) ,$$

$$\overline{P}_2 = \frac{-1}{2\pi k} \int_{B_H} q(x_1, x_2) \sin(\overline{x}_1 x_1 + \overline{x}_2 x_2)\, dx_1\, dx_2$$

$$= \frac{-\mu_f P_o V}{2\pi k} \int_{-a}^{a} \int_{-b}^{b} \sin(\overline{x}_1 x + \overline{x}_2 x)\, dx_2\, dx_1$$

$$= 0 .$$

Substituting the expression $\overline{P}_1$ into (61) and applying the inverse Fourier transform yields

$$\frac{\sigma_{11}^T}{\mu} = \frac{-4\mu_f P_o V}{\pi^2 k} \int_0^{\infty} \int_0^{\infty} f_1 \cos(\overline{x}_2 x_2) \left[e^{-\omega x_3} (b_1 D_1 + b_2 D_2) + e^{-s x_3} (b_3 D_1 + b_4 D_2) \right] d\overline{x}_1\, d\overline{x}_2 ,$$

$$\frac{\sigma_{22}^T}{\mu} = \frac{-4\mu_f P_o V}{\pi^2 k} \int_0^\infty \int_0^\infty f_1 \cos(\bar{x}_2 x_2) \left[e^{-\omega x_3} (b_5 D_1 + b_6 D_2) + e^{-sx_3} (b_7 D_1 + b_8 D_2) \right] d\bar{x}_1 \, d\bar{x}_2 ,$$

$$\frac{\sigma_{33}^T}{\mu} = \frac{-4\mu_f P_o V}{\pi^2 k} \int_0^\infty \int_0^\infty f_1 \cos(\bar{x}_2 x_2) \left[e^{-\omega x_3} (b_9 D_1 + b_{10} D_2) - e^{-sx_3} (b_{11} D_1 + b_{12} D_2) \right] d\bar{x}_1 \, d\bar{x}_2 ,$$

$$\frac{\sigma_{12}^T}{\mu} = \frac{-4\mu_f P_o V}{\pi^2 k} \int_0^\infty \int_0^\infty f_1 \sin(\bar{x}_2 x_2) \left[e^{-\omega x_3} (-b_{13} D_3 - b_{14} D_4) - \bar{x}_1 \bar{x}_2 \, e^{-sx_3} (b_{15} D_3 + b_{16} D_4) \right] d\bar{x}_1 \, d\bar{x}_2 ,$$

$$\frac{\sigma_{23}^T}{\mu} = \frac{-4\mu_f P_o V}{\pi^2 k} \int_0^\infty \int_0^\infty \bar{x}_2 f_1 \sin(\bar{x}_2 x_2) \left[e^{-\omega x_3} (b_{17} D_5 + b_{18} D_6) - e^{-sx_3} (b_{19} D_5 + b_{20} D_6) \right] d\bar{x}_1 \, d\bar{x}_2 ,$$

$$\frac{\sigma_{31}^T}{\mu} = \frac{-4\mu_f P_o V}{\pi^2 k} \int_0^\infty \int_0^\infty \bar{x}_1 f_1 \cos(\bar{x}_2 x_2) \left[e^{-\omega x_3} (b_{17} D_7 + b_{18} D_8) - e^{-sx_3} (b_{19} D_7 + b_{20} D_8) \right] d\bar{x}_1 \, d\bar{x}_2 , \tag{65}$$

in which

$$f_1 = -\frac{1}{\bar{x}_1\bar{x}_2}\sin(\bar{x}_1 a)\sin(\bar{x}_2 b) ,$$

$$D_1 = -\frac{1}{\omega^2+\theta^2}\left[\omega\cos(\bar{x}_1 x_1) + \frac{n}{2\omega}\sin(\bar{x}_1 x_1)\right] ,$$

$$D_2 = \frac{1}{\omega^2+\theta^2}\left[\theta\cos(\bar{x}_1 x_1) - \frac{n}{2\theta}\sin(\bar{x}_1 x_1)\right] ,$$

$$D_3 = -\frac{1}{\omega^2+\theta^2}\left[\omega\sin(\bar{x}_1 x_1) + \frac{n}{2\omega}\cos(\bar{x}_1 x_1)\right] ,$$

$$D_4 = \frac{1}{\omega^2+\theta^2}\left[\theta\sin(\bar{x}_1 x_1) - \frac{n}{2\theta}\cos(\bar{x}_1 x_1)\right] ,$$

$$D_5 = \frac{1}{\omega^2+\theta^2}\left[-\frac{n}{2\omega}\sin(\bar{x}_1 x_1) + \omega\cos(\bar{x}_1 x_1)\right] ,$$

$$D_6 = -\frac{1}{\omega^2+\theta^2}\left[\frac{n}{2\theta}\sin(\bar{x}_1 x_1) + \theta\cos(\bar{x}_1 x_1)\right] ,$$

$$D_7 = \frac{1}{\omega^2+\theta^2}\left[\frac{n}{2\omega}\cos(\bar{x}_1 x_1) - \omega\sin(\bar{x}_1 x_1)\right] ,$$

$$D_8 = \frac{1}{\omega^2+\theta^2}\left[\frac{n}{2\theta}\cos(\bar{x}_1 x_1) + \theta\sin(\bar{x}_1 x_1)\right] .$$

Due to the complexity of the expressions, no existing automatic integration scheme for the above integrals are efficient. Hence the Gaussian-Laguerre quadrature formulas are used for the numerical approximation.

4.2 A Moving Disk of Uniform Pressure (Case 2)

Mechanical Stress Field

The pressure distributions are assumed to be of the form

$$\sigma_{33} = -R_3(x_1, x_2, 0) , \quad \sigma_{32} = -R_2 = 0 , \quad \sigma_{31} = -R_1(x_1, x_2, 0)$$

where

$$R_3 = \begin{cases} P_o , & \gamma^2 = x_1^2 + x_2^2 \leq a^2 \\ 0 , & \text{elsewhere} \end{cases} ,$$

$$R_1 = -\mu_f R_3 .$$

The transformed boundary conditions can be obtained by using Equation (3).

$$\overline{R}_3(\overline{x}_1, \overline{x}_2, 0) = \frac{P_o}{2\pi} \int_{-a}^{a} \int_{-[a^2-x_1^2]^{1/2}}^{[a^2-x_1^2]^{1/2}} e^{i(\overline{x}_1 x_1 + \overline{x}_2 x_2)} \, dx_2 \, dx_1$$

$$= \frac{P_o}{2\pi} \int_0^a \gamma d\gamma \int_0^{2\pi} e^{is\gamma \cos(\theta-\phi)} \, d\theta$$

$$= P_o \int_0^a \gamma J_o(s\gamma) \, d\gamma$$

$$= \frac{aP_o}{s} J_1(sa) ,$$

$$\overline{R}_1 = -\mu_f \overline{R}_3 , \quad \overline{R}_2 = 0 .$$

Following the same procedure as in Case 1, expressions are obtained for the stress components of the forms

$$\sigma_{11}^{n} = \frac{aP_o}{\pi} \int_0^{\pi} \frac{\cos^2 \phi}{H} [\gamma_3(1 + \tfrac{1}{2} M_2^2 - M_1^2) S_1' - \gamma_1\gamma_2 S_2'] \, d\phi ,$$

$$\sigma_{22}^{n} = \frac{aP_o}{\pi} \int_0^{\pi} \frac{1}{H} \{[\gamma_3(\tfrac{1}{2} \beta^2 - 1) M_1^2 \cos^2 \phi + \sin^2 \phi] \cdot S_1' - \gamma_1\gamma_2 \sin^2 \phi \, S_2'\} \, d\phi ,$$

$$\sigma_{33}^{n} = \frac{-aP_o}{\pi} \int_0^{\pi} \frac{1}{H} [\gamma_3^2 S_1' - \gamma_1\gamma_2 S_2'] \, d\phi ,$$

$$\sigma_{12}^{n} = \frac{aP_o}{2\pi} \int_0^{\pi} \frac{\sin 2\phi}{H} [\gamma_3 S_1' - \gamma_1\gamma_2 S_2'] \, d\phi ,$$

$$\sigma_{23}^{n} = \frac{-aP_o}{\pi} \int_0^{\pi} \frac{\gamma_1\gamma_3 \sin \phi}{H} [W_1' - W_2'] \, d\phi ,$$

$$\sigma_{31}^{n} = \frac{-aP_o}{\pi} \int_0^{\pi} \frac{\gamma_1\gamma_3 \cos \phi}{H} [W_1' - W_2'] \, d\phi ,$$

$$\sigma_{11}^{f} = \frac{-aP_o}{\pi} \int_0^{\pi} \frac{\cos \phi}{H} \left\{ \gamma_2 \cos^2 \phi (1 + \tfrac{1}{2} M_2^2 - M_1^2) W_1' - \left[\frac{(\gamma_3 - 2\gamma_1\gamma_2)}{\gamma_2} \sin^2 \phi + \gamma_2\gamma_3 \right] W_2' \right\} d\phi ,$$

$$\sigma_{22}^{f} = \frac{-aP_o}{\pi} \int_0^{\pi} \frac{\cos \phi}{H} \left\{ \gamma_2 [(\tfrac{1}{2} \beta^2 - 1) M_1^2 \cos^2 \phi + \sin^2 \phi] W_1' + \left[\frac{(\gamma_3 - 2\gamma_1\gamma_2)}{\gamma_2} \sin^2 \phi \right] W_2' \right\} d\phi ,$$

$$\sigma_{33}^f = \frac{-aP_o}{\pi} \int_0^\pi \frac{\gamma_2 \cos\phi}{H} \{[(\tfrac{1}{2}\beta^2 - 1) M_1^2 \cos^2\phi - \gamma_1^2] W_1' + \gamma_3 W_2'\} \, d\phi ,$$

$$\sigma_{12}^f = \frac{-aP_o}{\pi} \int_0^\pi \frac{\gamma_2 \sin\phi}{H} \left\{ \cos^2\phi \, W_1' - \frac{1}{2}\left[\frac{(\gamma_3 - 2\gamma_1\gamma_2)}{\gamma_2^2}(\sin^2\phi - \cos^2\phi) + \gamma_3\right] W_2' \right\} d\phi ,$$

$$\sigma_{23}^f = \frac{-aP_o}{2\pi} \int_0^\pi \frac{\sin 2\phi}{H} \gamma_1\gamma_2 [S_1' - S_2'] \, d\phi ,$$

$$\sigma_{31}^f = \frac{-aP_o}{\pi} \int_0^\pi \frac{1}{H} [\gamma_1\gamma_2 \cos^2\phi \, S_1' - (\gamma_3^2 - \gamma_1\gamma_2 \sin^2\phi) S_2'] \, d\phi , \qquad (66)$$

where

$$S_t' = \int_0^\infty J_1(sa) \cos(s\gamma \cos(\theta - \phi)) \, e^{-s\gamma_t x_3} \, ds ,$$

$$W_t' = \int_0^\infty J_1(sa) \sin(s\gamma \cos(\theta - \phi)) \, e^{-s\gamma_t x_3} \, ds ,$$

$$t = 1,2 .$$

The integrals for S_t' and W_t' can be solved analytically so that the stress expressions have the form of single integrals which can be evaluated numerically.

Thermal Stress Field

$\overline{P}_1$ and $\overline{P}_2$ are given by

$$\overline{P}_1 = \frac{-\mu_f P_o V}{2\pi k} \int_{-a}^{a} \int_{-[a^2-x_1^2]^{1/2}}^{[a^2-x_1^2]^{1/2}} \cos(\overline{x}_1 x_1 + \overline{x}_2 x_2)\, dx_2\, dx_1$$

$$= \frac{-\mu_f P_o V}{2\pi k} \operatorname{Re} \int_{-a}^{a} \int_{-[a^2 - x_1^2]^{1/2}}^{[a^2-x_1^2]^{1/2}} e^{i(\overline{x}_1 x_1 + \overline{x}_2 x_2)}\, dx_2\, dx_1$$

$$= \frac{-\mu_f P_o V}{k} \cdot \frac{a J_1(sa)}{s} ,$$

$$\overline{P}_2 = \frac{-\mu_f P_o V}{2\pi k} \int_{-a}^{a} \int_{-[a^2-x_1^2]^{1/2}}^{[a^2-x_1^2]^{1/2}} \sin(\overline{x}_1 x_1 + \overline{x}_2 x_2)\, dx_2\, dx_1$$

$$= \frac{-\mu_f P_o V}{\pi k} \int_{-a}^{a} \sin(\overline{x}_1 x_1) \sin\left(\overline{x}_2 \sqrt{a^2 - x_1^2}\right) dx_1$$

$$= 0 .$$

Substitution of $\overline{P}_1$ into (61) and again application of the inverse transform results in

$$\frac{\sigma_{11}^T}{\mu} = \frac{-2\mu_f P_o V}{\pi^2 k} \int_0^{\infty} \int_0^{\infty} f_2 \cos(\overline{x}_2 x_2) \left[e^{-\omega x_3} (b_1 D_1 + b_2 D_2) + e^{-s x_3} (b_3 D_1 + b_4 D_2) \right] d\overline{x}_1\, d\overline{x}_2 ,$$

$$\frac{\sigma_{22}^T}{\mu} = \frac{-2\mu_f P_o V}{\pi^2 k} \int_0^\infty \int_0^\infty f_2 \cos(\bar{x}_2 x_2) \left[e^{-\omega x_3} (b_5 D_1 + b_6 D_2) + e^{-sx_3} (b_7 D_1 + b_8 D_2) \right] d\bar{x}_1 \, d\bar{x}_2 ,$$

$$\frac{\sigma_{33}^T}{\mu} = \frac{-2\mu_f P_o V}{\pi^2 k} \int_0^\infty \int_0^\infty f_2 \cos(\bar{x}_2 x_2) \left[e^{-\omega x_3} (b_9 D_1 + b_{10} D_2) - e^{-sx_3} (b_{11} D_1 + b_{12} D_2) \right] d\bar{x}_1 \, d\bar{x}_2 ,$$

$$\frac{\sigma_{12}^T}{\mu} = \frac{-2\mu_f P_o V}{\pi^2 k} \int_0^\infty \int_0^\infty f_2 \sin(\bar{x}_2 x_2) \left[e^{-\omega x_3} (-b_{13} D_3 - b_{14} D_4) - \bar{x}_1 \bar{x}_2 \, e^{-sx_3} (b_{15} D_3 + b_{16} D_4) \right] d\bar{x}_1 \, d\bar{x}_2 ,$$

$$\frac{\sigma_{23}^T}{\mu} = \frac{-2\mu_f P_o V}{\pi^2 k} \int_0^\infty \int_0^\infty \bar{x}_2 f_2 \sin(\bar{x}_2 x_2) \left[e^{-\omega x_3} (b_{17} D_5 + b_{18} D_6) - e^{-sx_3} (b_{19} D_5 + b_{20} D_6) \right] d\bar{x}_1 \, d\bar{x}_2 ,$$

$$\frac{\sigma_{31}^T}{\mu} = \frac{-2\mu_f P_o V}{\pi^2 k} \int_0^\infty \int_0^\infty \bar{x}_1 f_2 \cos(\bar{x}_2 x_2) \left[e^{-\omega x_3} (b_{17} D_7 + b_{18} D_8) - e^{-sx_3} (b_{19} D_7 + b_{20} D_8) \right] d\bar{x}_1 \, d\bar{x}_2 , \tag{67}$$

where

$$f_2 = \frac{aJ_1(sa)}{s} .$$

4.3 A Moving Disk of Non-Uniform Pressure (Case 3)

Mechanical Stress Field

The traction boundary conditions are

$$\sigma_{33} = -R_3(x_1, x_2, 0) , \quad \sigma_{32} = -R_2 = 0 , \quad \sigma_{31} = -R_1(x_1, x_2, 0)$$

where

$$R_3 = \begin{cases} 2P_0(1 - r^2/a^2) , & x_1^2 + x_2^2 \le a^2 \\ 0 , & \text{elsewhere} \end{cases}$$

$$\bar{R}_3(\bar{x}_1, \bar{x}_2, 0) = \frac{P_0}{\pi} \int_{-a}^{a} \int_{-[a^2-x_1^2]^{1/2}}^{[a^2-x_1^2]^{1/2}} (1 - r^2/a^2)\, e^{i(\bar{x}_1 x_1 + \bar{x}_2 x_2)}\, dx_2\, dx_1$$

$$= \frac{P_0}{\pi} \int_0^a \int_0^{2\pi} (1 - r^2/a^2)\, e^{isr\cos(\theta-\phi)}\, r\, dr\, d\theta$$

$$= \frac{4P_0 J_2(sa)}{s^2} ,$$

$$\bar{R}_1 = -\mu_f \bar{R}_3 , \qquad \bar{R}_2 = 0 .$$

The expressions of the stress components are similar to those (66) in Case 2 except S_t' and W_t' being replaced by S_t'' and W_t'' which are of the forms

$$S_t'' = 4\int_0^\infty \frac{J_2(sa)}{s} \cos(s\gamma \cos(\theta - \phi))\, e^{-s\gamma_t x_3}\, ds ,$$

$$W_t'' = 4\int_0^\infty \frac{J_2(sa)}{s} \sin(s\gamma \cos(\theta - \phi))\, e^{-s\gamma_t x_3}\, ds ,$$

$$t = 1,2 .$$

Again S_t'' and W_t'' can be solved analytically and accordingly numerical results of the stress components can be readily obtained by automatic integration schemes for single integrals.

Thermal Stress Field

It is found that

$$\bar{P}_1 = \frac{-\mu_f P_o V}{\pi k}\int_{-a}^{a}\int_{-[a^2-x_1^2]^{1/2}}^{[a^2-x_1^2]^{1/2}} \left(1 - \frac{\gamma^2}{a^2}\right) \cos(\bar{x}_1 x_1 + \bar{x}_2 x_2)\, dx_2\, dx_1$$

$$= \frac{-4\mu_f P_o V}{k}\frac{J_2(sa)}{s^2} ,$$

$$\bar{P}_2 = 0 .$$

The thermal stress field can be obtained by replacing f_2 in (67) with f_3 which has the following form

$$f_3 = \frac{4J_2(sa)}{s^2} .$$

As an illustration of the numerical evaluation of the integrals, graphical results are presented in dimensionless form.

The coordinates are normalized by the half width of the asperity (a), such that $(\xi, \eta, \zeta) = (x_1/a, x_2/a, x_3/a)$. The stress components are normalized by the average pressure p_o, $\sigma^*_{ij} = \sigma_{ij}/p_o$. The temperature rise from the cold state is $\phi = Tk/q_o a$, where q_o is the heat flux due to the average frictional load, that is, $q_o = \mu_f p_o V$. Figures 3-4 show the mechanical principal stresses on the trailing side with different depths, ζ, for Cases 1 and 2, respectively. It is noticed that stresses rise sharply in the neighborhood of $\xi = 1$, as ζ approaches zero. Such stress singularities at $\xi = \pm 1$ are expected owing to the discontinuities of the loading conditions. Temperature fields for different cases are shown in Figures 5-7, in which the temperature decays rapidly with respect to the depth. Consequently, the stress component σ_{11} is compressive only in a very thin surface layer due to the thermal effect. Its magnitude of compressive stress also decreases rapidly with increase of depth, until finally it becomes tensile. The consequential effect shown in Figure 8 that the maximum tensile thermal principal stress is at $\zeta = 10^{-1}$ and of considerable magnitude. It should be noted that the difference between the magnitude of the thermal stresses (Fig. 8 here and that in [6]) is due to $\bar{\sigma}_{\xi\xi}$ in [6] being the dimensionless normal stress instead of the principal stress. The combined stress field is represented by the maximum principal stress, shown in Figure 9 for several depths in the near-surface region. Observe the the Fig. 9 in [6] and that in this paper show the difference only of order 2. It is attributed to the difference of 2-D and 3-D analyses. The critical asperity pressure is purposely chosen to be the same (365 MPa). To initiate crack, the asperity travels at 15 m/s (~600 ips) in the 2-D case, while the traverse speed has only to be 10 m/s (~400 ips) in the 3-D case.

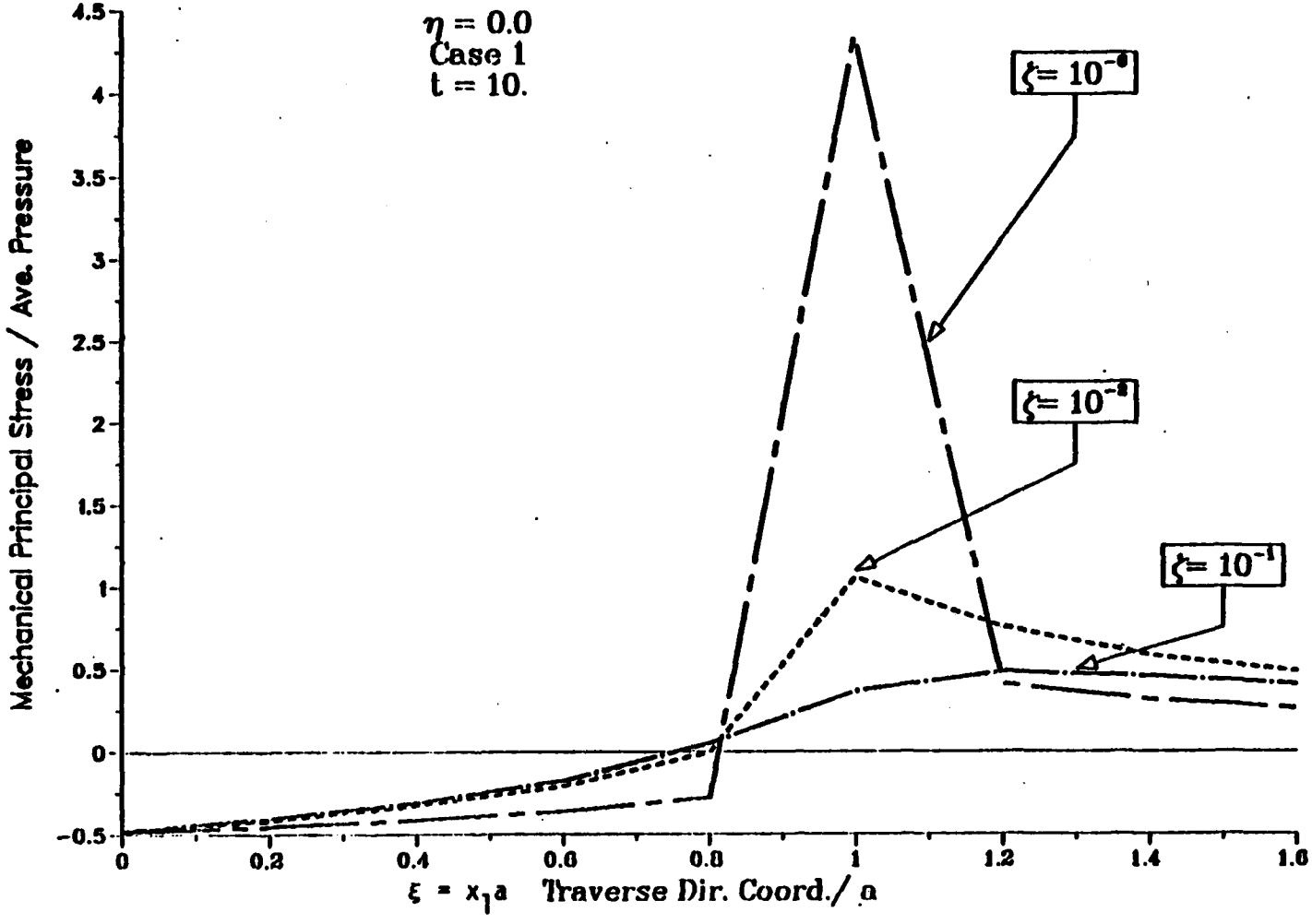

Figure 3. Maximum mechanical principal stresses in the surface layer (Case 1).

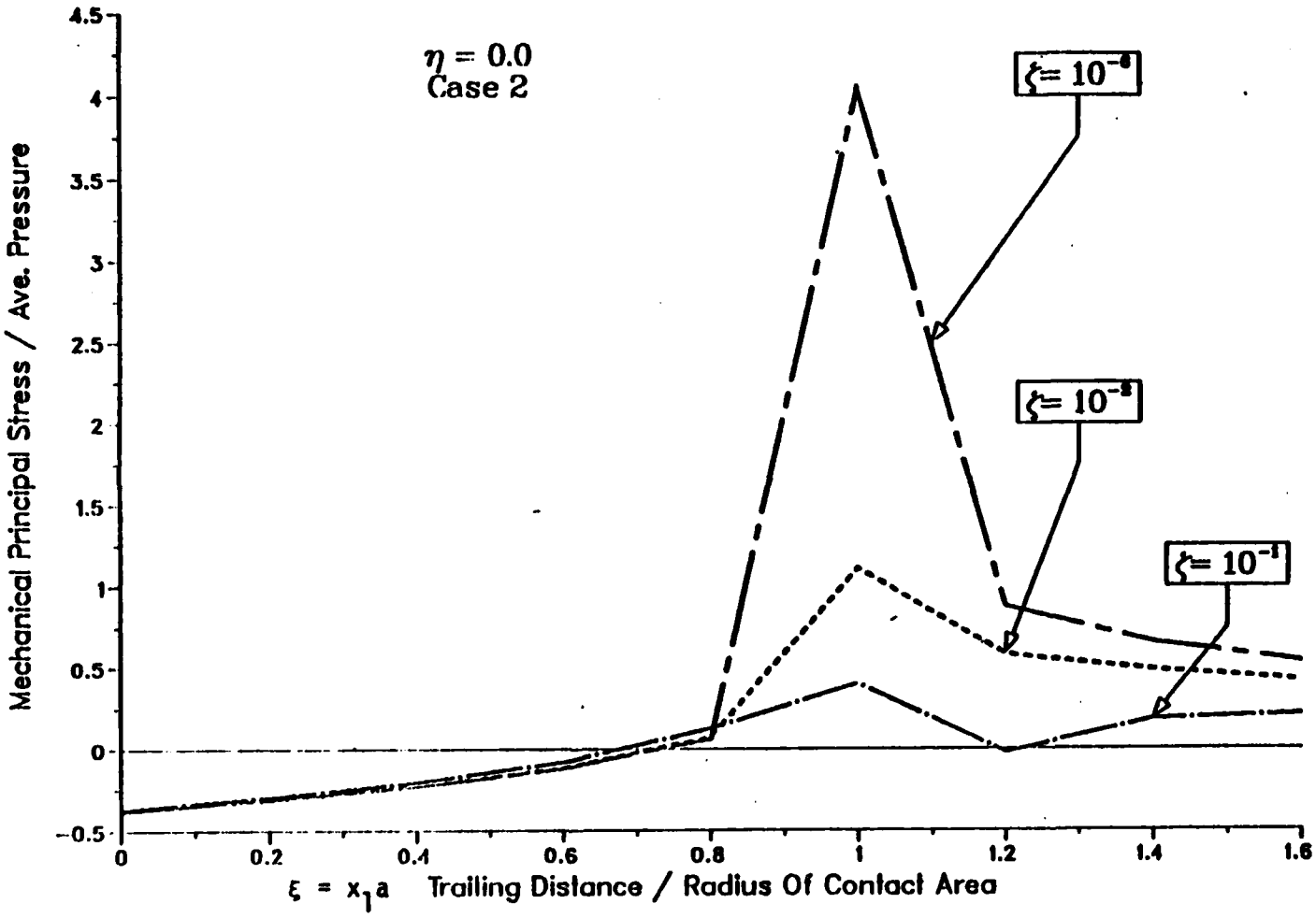

Figure 4. Maximum mechanical principal stresses in the surface layer (Case 2).

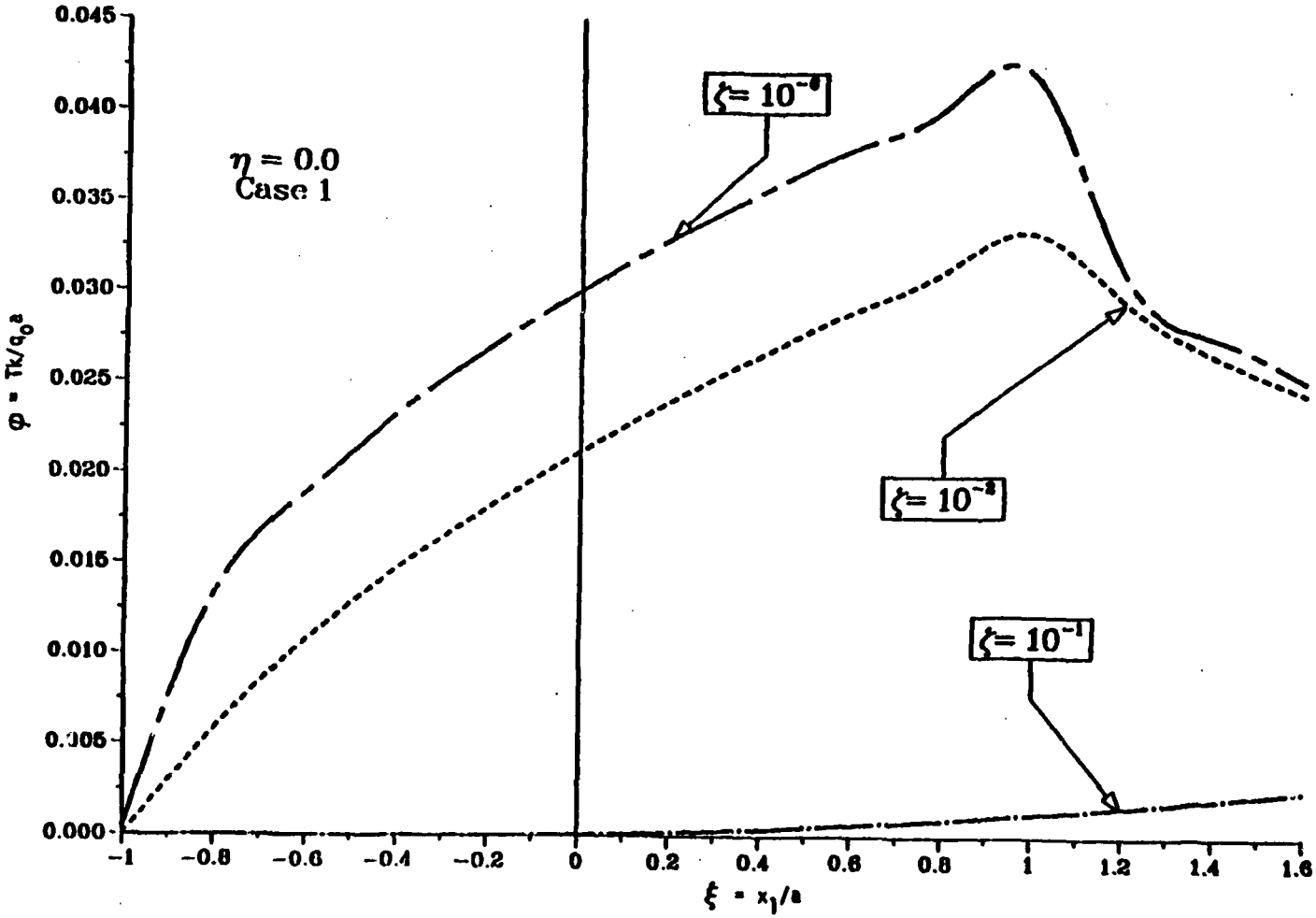

Figure 5. Temperature field in the surface layer (Case 1).

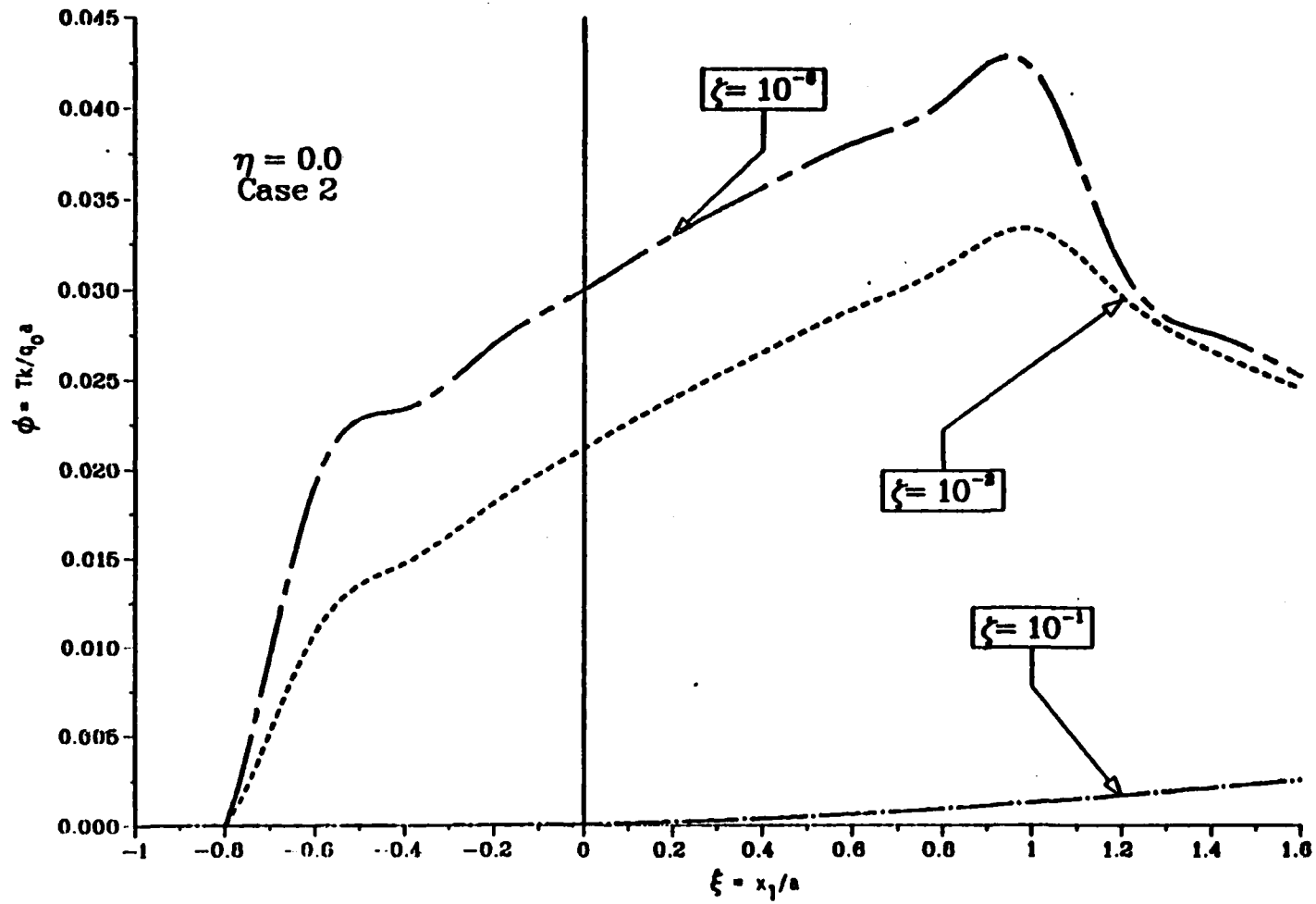

Figure 6. Temperature field in the surface layer (Case 2).

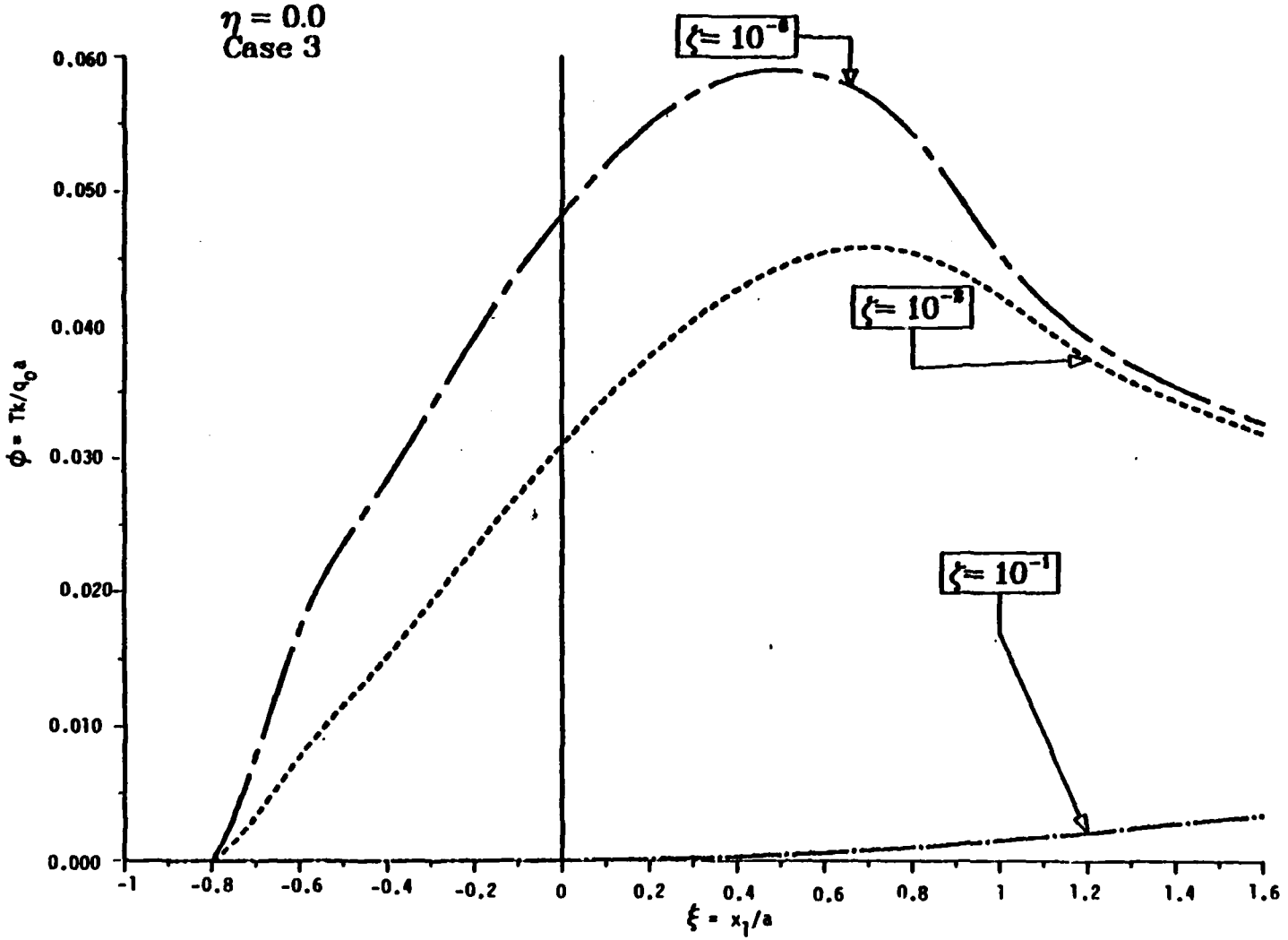

Figure 7. Temperature field in the surface layer (Case 3).

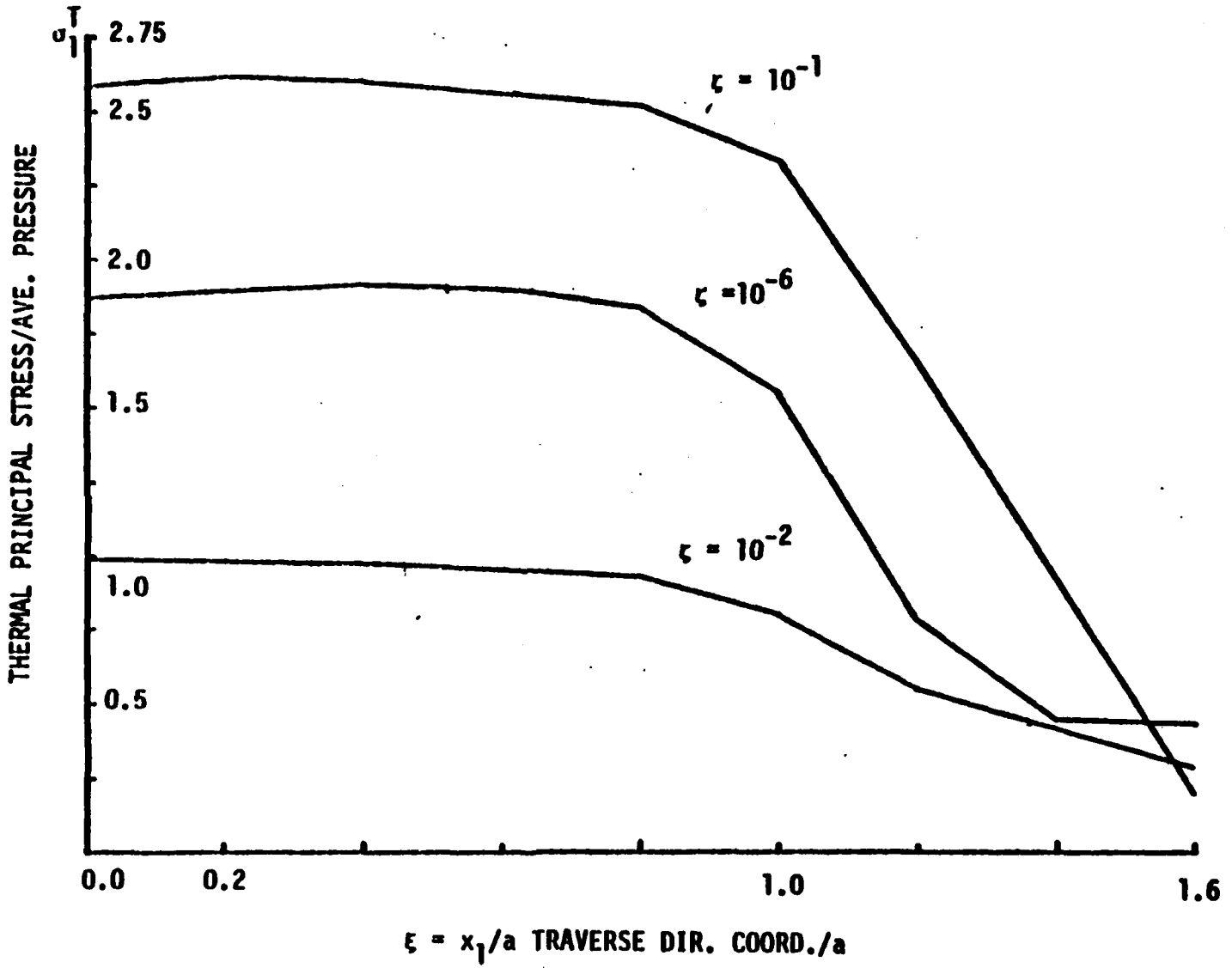

Figure 8. Maximum thermal principal stress in the surface layer (Case 1).

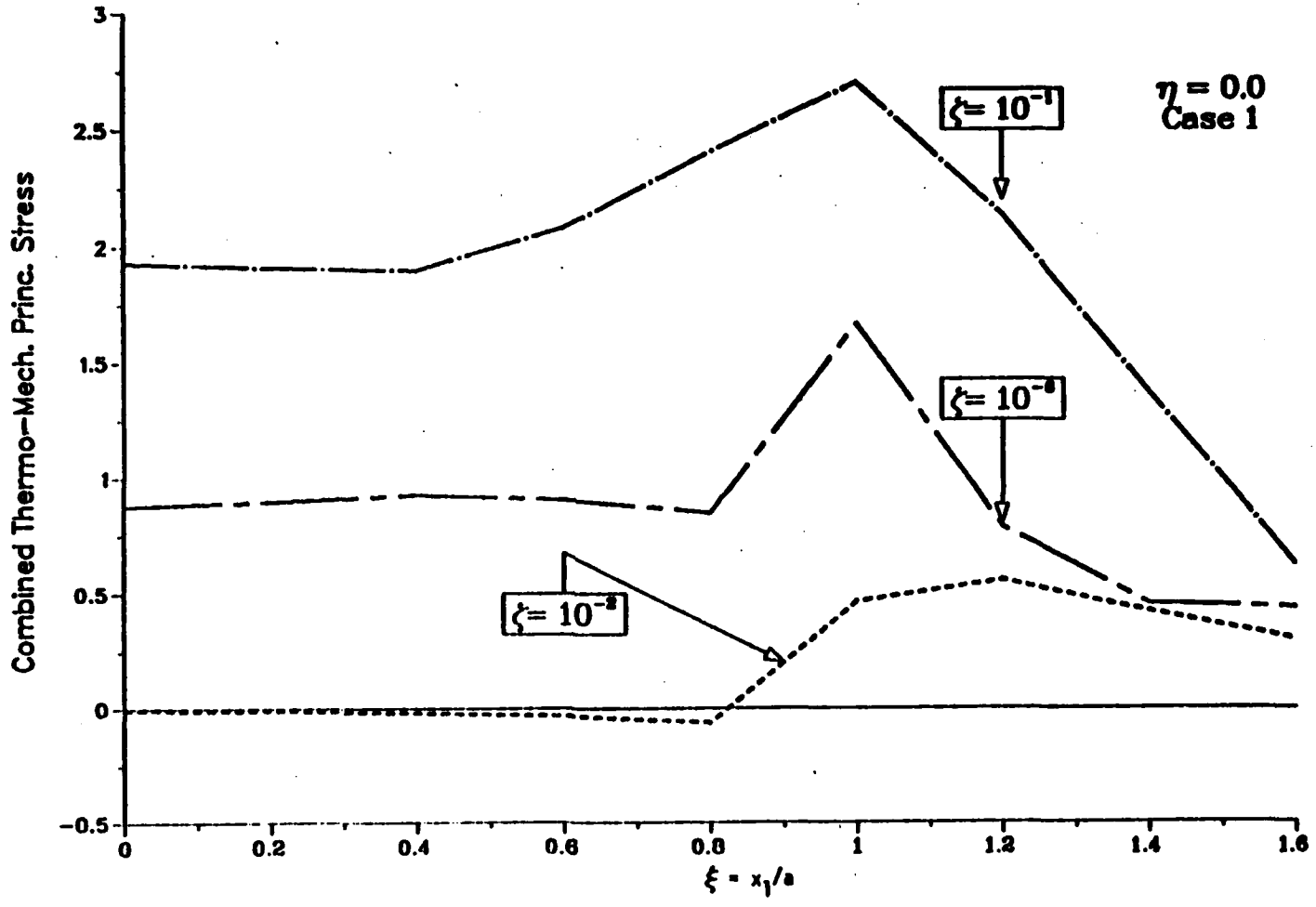

Figure 9. Maximum thermal mechanical principal stress in the surface layer (Case 1).

5.0 CONCLUSION

The paper developes the general mathematical model in three-dimensional formulation to simulate the thermomechanical effect near the seal surface as a result of a single moving asperity. In the general solution, there is no restriction to the traverse and rubbing speeds of the surface, that is the traverse speed of the asperity may not be tied to any of the mating surfaces of the seal assembly. The contact areas by postulation of the present analysis have the shape of rectangular or circular regions. However, as evidenced from the results of uniform force distributions over rectangular and circular areas, the shape of the contact area is not that critical. With reference to Figure 5, the maximum temperature of $\phi = 40 \times 10^{-3}$ corresponds to 800°C in a steel based seal subjected to an asperity pressure of 365 MPa (53,000 psi) traversing at a speed of 10 m/s (400 ips). The same temperature may of course be attained with a lower asperity pressure of 240 MPa (35,000 psi) but traversing at a speed of 15 m/s (600 psi). The high temperature is maintained only near the surface but *drop off* at $\zeta = 10^{-1}$. For the data used, the thermal boundary layer is at most of the order of 100 microns. In the present analysis, it is postulated that the mechanical properties of the seal material remain unchanged for all temperature levels during the loading. For those seal materials that may change their mechanical properties at the high temperatures near the boundary, the boundary layer analysis needs to be considered. It is not unexpected that the maximum tensile stress should occur at the thermal layer interface. The subsurface initiation of fracture is also found in the two-dimensional model at a depth of one-twentieth of the asperity width [7]. The average friction required for fracture initiation is still high. It corresponds to a pressure around 240 MPa (35,000 psi) in Figure 9, and a high Coulomb coefficient of friction $\mu_f = 0.5$.

REFERENCES

1. Archard, J. F., "The temperature of rubbing surfaces," Wear, Vol. 2, 6 (1959), pp. 438-455.

2. Burton, R. A., "Thermomechanical effects in sliding wear," Workshop on Frictionally Induced Thermal Deformation and Wear, Annapolis, MD, June 19-20, 1979.

3. Naumann, F. K. and Spies, F., "Grinding Cracks" (pp. 228-233), "Cracks Due to Frictional Heating" (pp. 337-340), Source Book in Failure Analysis, ASM, 1974.

4. Kennedy, F. E., Jr. and Karpe, S. A., "Thermocracking of a mechanical face seal," Wear, Vol. 79 (1982), pp. 21-36.

5. Burton, R. A., "Friction and Wear," Chap. 2, Tribology, ed. A. Z. Saeri, McGraw-Hill, 1980, pp. 17-38.

6. Ju, F. D. and Huang, J. H., "Heat cracking in the contact zone of a bearing seal (a two-dimensional model of a single moving asperity)," Wear, Vol. 79, (1982), pp. 107-118.

7. Kennedy, F. E., Grim, J. N. and Glovsky, R. P., "Factors Influencing Thermomechanical Failure of Face Seals, II," Interim Report No. 2 (ONR Contract No. N00014-81-K-0090) Jan. 1983, Thayer School of Engineering, Dartmouth College, Hanover, NH.

8. Burton, R. A., "Thermal Deformation in Frictionally Heated Contact," Thermal Deformation in Frictionally Heated Systems, Ed., R. A. Burton, Elsevier Sequoia (1980), pp. 1-20.

9. Marscher, W. D., "A phenomenological model of abradable wear in high performance turbomachinery," Wear, Vol. 59, (1980), pp. 191-211.

10. Marscher, W. D., "Thermal versus mechanical effects in high speed sliding," Wear, Vol. 79, (1982), pp. 129-143.

11. Eason, G., "The stresses produced in a semi-infinite solid by a moving surface force," Int. J. Engng Sci., Vol. 2, (1965), pp. 581-609.

Distribution List

Recipient (Government)	Number of Copies
Materials Division (Code 431) Engineering Sciences Directorate Office of Naval Research 800 N. Quincy Street Arlington, VA 22217	(2)
Mechanics Division (Code 432) Engineering Sciences Directorate Office of Naval Research 800 N. Quincy Street Arlington, VA 22217	(2)
Defense Documentation Center Building 5, Cameron Station Alexandria, VA 22314	(12)
Technical Information Division Naval Research Laboratory 4555 Overlook Avenue, SW Washington, DC 20375	(6)
Division of Weapons & Engineering U.S. Naval Academy Annapolis, MD 21402	(1)
Comandant of the Marine Corps (Code LMM-3) Headquarters, U.S. Marine Corps Washington, DC 20380	(1)
Office of Naval Research Attn: Code 100M 800 N. Quincy Street Arlington, VA 22217	(1)
DTNSRDC Mr. R. G. Brown (Code 2382) Annapolis, MD 21402	(1)
Air Force Wright Aeronautical Laboratories Wright-Patterson Air Force Base Attn: Dr. J. Dill, POSL 1 WPAFB, OH 45433	(1)
Naval Air Propulsion Center A. J. D'Orazio, Code PE-72 Trenton, NJ 08628	(1)

Distribution List (continued)

Recipient (Government)	Number of Copies
DTNSRDC Attn: Mr. Jim Dray (Code 2832) Annapolis, MD 21402	(1)
Naval Sea Systems Command Attn: Mr. Richard R. Graham, II Code 56X43, Bldg. NC 4, Room 374 Washington, DC 20362	(1)
DTNSRDC Attn: Mr. Al Harbage, Jr. (Code 2723) Annapolis, MD 21402	(1)
Naval Sea Systems Command Attn: Mr. Martin Kandl (Code 56X31) Washington, DC 20362	(1)
David W. Taylor Naval Ship R&D Center Attn: S. Karpe Ship Materials Engineering Department Annapolis, MD 21402	(1)
Army Materials and Mechanics Research Center Attn: Dr. R. N. Katz Watertown, MA 02172	(1)
Naval Air Engineering Center Attn: L. Kociuba, Code 92A3 Lakehurst, NJ 08733	(1)
Naval Air Systems Command Attn: AIR-4111C (CDR A. H. Robbins) Washington, DC 20361	(1)
Army Research Office Attn: Dr. George Mayer P.O. Box 12211 Research Triangle Park, NC 27709	(1)
Army Research Office Attn: Dr. Fred Schmiedeshoff P.O. Box 12211 Research Triangle Park, NC 27709	(1)

Distribution List (continued)

Recipient (Government)	Number of Copies
Air Force Wright Aeronautical Laboratories Wright-Patterson Air Force Base Attn: B. D. McConnell - MLBT WPAFB, OH 45433	(1)
U.S. Army MERDC Attn: W. McGovern Fort Belvoir, VA 22060	(1)
Naval Air Development Center Attn: D. V. Minuti (Code 606B) Warminster, PA 18974	(1)
Naval Research Laboratory Attn: Dr. James D. Murday (Code 6170) Washington, DC 20375	(1)
DTNSRDC Attn: Mr. A. B. Neild, Jr. (Code 2723) Annapolis, MD 21402	(1)
NASA-Lewis Research Center Attn: Mr. Jim Kiraly (MS 23-2) 21000 Brookpark Road Cleveland, OH 44135	(1)
NASA-Lewis Research Center Attn: Dr. L. Wedevan (MS 23-2) 21000 Brookpark Road Cleveland, OH 44135	(1)
NASA-Lewis Research Center Attn: Dr. D. Buckley (MS 23-2) 21000 Brookpark Road Cleveland, OH 44135	(1)
DTNSRDC Attn: Dr. Earl Quandt, Jr. Annapolis, MD 21402	(1)
Naval Air Systems Command Attn: R. Schmidt, AIR-311A Washington, DC 20361	(1)
Naval Air Systems Command Attn: Dr. R. Schumaker, AIR-340 Washington, DC 20361	(1)

Distribution List (continued)

Recipient (Government)	Number of Copies
Office of Naval Research Attn: David S. Siegel (Code 260) 800 N. Quincy Street Arlington, VA 22217	(1)
Naval Air Development Center Attn: L. Stallings (Code 6061) Warminster, PA 18974	(1)
Defense Advanced Research Project Agency Attn: Capt. S. Wax 1400 Wilson Blvd. Arlington, VA 22209	(1)
Naval Sea Systems Command Attn: Dr. Frank Ventriglio (Code 05R) Washington, DC 20362	(1)
Naval Air Systems Command Attn: P. Weinberg, AIR-5304C1 Washington, DC 20361	(1)
Marine Corps Development Center Mobility and Logistics Division Head, Motor Transportation Branch Quantico, VA 22134	(1)
Commanding General (Code D 074) Marine Corps Development and Education Command Quantico, VA 22135	(1)
Naval Research Laboratory Attn: Dr. Irwin L. Singer (Code 6176) Washington, DC 20375	(1)
Air Force Wright Aeronautical Laboratories Wright Patterson Air Force Base Attn: C. E. Snyder - MLBT WPAFB, OH 45433	(1)

Distribution List (continued)

Recipient (University/Others)	Number of Copies
M. J. Devine General Technology 2560 Prescott Road Havertown, PA 19083	(1)
E. L. Courtright Battelle Memorial Institute Pacific Northwest Laboratories Richland, WA 99352	(1)
Dr. A. W. Ruff Metallurgy Division National Bureau of Standards Washington, DC 20234	(1)
Dr. N. P. Suh Massachusetts Institute of Technology Department of Mechanical Engineering Cambridge, MA 02139	(1)
Dr. Fred J. Tribe Admiralty Marine Technology Establishment Holten Heath, Poole, Dorset U.K. BH166JU	(1)
Dr. R. D. Arnell Department of Aeronautical and Mechanical Engineering University of Salford Salford, U.K. M54WT	(1)
Professor K. Ludema Department of Mechanical Engineering University of Michigan Ann Arbor, MI 48105	(1)
Professor W. Kenneth Stair Associate Dean for Research University of Tennessee Knoxville, TN 37996	(1)
Prof. Heinz G.F. Wilsdorf Department of Materials Science University of Virginia Charlottesville, VA 22901	(1)

Distribution List (continued)

Recipient (University/Others)	Number of Copies
Dr. Richard Jentgen Battelle Columbus Laboratories 505 King Avenue Columbus, OH 43201	(1)
Mr. William Glaeser Battelle Columbus Laboratories 505 King Avenue Columbus, OH 43201	(1)
BHRA Fluid Engineering Attn: Dr. Bernard S. Nau Cranfield, Bedford England MK430AJ	(1)
Franklin Research Institute Attn: Mr. Stuart Gassel 20th and Race Street Philadelphia, PA 19103	(1)
Wear Sciences Attn: Mr. Marshall Peterson 925 Mallard Circle Arnold, MD 21012	(1)
Westinghouse R&D Center Attn: Dr. Ian McNab 1310 Beulah Road Pittsburgh, PA 15235	(1)
Mr. Edward L. Wiehe TRW, Inc. 1 Space Park Redondo Beach, CA 90278	(1)
Professor Ralph A. Burton Chairman, Mechanical and Aerospace Engineering Department North Carolina State University 3211 Broughton Hall Raleigh, NC 27650	(1)
Professor N. S. Eiss, Jr. Department of Mechanical Engineering Virginia Polytechnic Institute and State University Blacksburg, VA 24061	(1)

Distribution List (continued)

Recipient (University/Others)	Number of Copies
Professor I. Etsion Department of Mechanical Engineering Technion, Haifa Israel	(1)
Professor Hasselman Virginia Polytechnic Institute Department of Materials Engineering Blacksburgh, VA 24061	(1)
Professor William F. Hughes Mechanical Engineering Department Carnegie Mellon University Pittsburgh, PA 15213	(1)
Professor T. Keith Department of Mechanical Engineering University of Toledo Toledo, OH 43606	(1)
Professor Francis E. Kennedy, Jr. Thayer School of Engineering Darthmouth College Hanover, NH 03755	(1)
Professor Alan O. Lebeck Bureau of Engineering Research University of New Mexico Albuquerque, NM 87131	(1)
Professor Fred F. Ling Department of Mechaical Engineering Rensselaer Polytechnic Institute Troy, NY 12181	(1)
Dr. Thomas Dow North Carolina State University Mechanical and Aerospace Engineering Department Raleigh, NC 27650	(1)
Dr. Doris Kuhlmann-Wilsdorf University of Virginia Department of Materials Science Charlottesville, VA 22901	(1)

Distribution List (continued)

Recipient (University/Others)	Number of Copies
Dr. David A. Rigney Ohio State University 116 W. 19th Avenue Department of Metallurgical Engineering Columbus, OH 43210	(1)
Dr. D. L. Taylor Cornell University Mechanical and Aerospace Engineering Ithaca, NY 14853	(1)
Dr. P. W. Whaley University of Nebraska 223 Bancroft Building Lincoln, NB 68588	(1)
Dr. C. Cusano University of Illinois Mechanical Engineering Dept. 1206 W. Green Street Urbana, IL 61801	(1)
Dr. Robert Maurer SKF Technology Services P.O. Box 515 1100 First Ave. King of Prussia, PA 19406	(1)
Dr. Charles F. Fisher, Jr. Engr. Experimental Station University of Tennessee Knoxville, TN 37996	(1)
Westinghouse R&D Center Attn: Mr. O. S. Taylor 1310 Beulah Road Pittsburgh, PA 15235	(1)
Westinghouse R&D Center Attn: Dr. P. Reichner 1310 Beulah Road Pittsburgh, PA 15235	(1)

END

FILMED

9-83

DTIC